# Feedback Algorithm and Web-Server for Protein Structure Alignment

Zhiyu Zhao[1], Bin Fu[2], Francisco J. Alanis[2] and Christopher M. Summa[1]

[1]Department of Computer Science, University of New Orleans, New Orleans, LA 70148, USA

zzha2@cs.uno.edu, csumma@cs.uno.edu

[2]Department of Computer Science, University of Texas–Pan American, Edinburg, TX 78539, USA

binfu@cs.panam.edu, fjalanis@gmail.com

**Abstract**

We have developed a feedback algorithm for protein structure alignment that uses a series of phases to improve the global alignment between two protein backbones. The method implements a self-improving learning strategy by sending the output of one phase, the global alignment, to the next phase as an input. A web portal implementing this method has been constructed and is freely available for use at http://fpsa.cs.uno.edu/. Based on hundreds of test cases, we compare our algorithm with three other, commonly used methods: CE, Dali and SSM. Our results show that in most cases our algorithm outputs a larger number of aligned positions when the ($C_\alpha$) $RMSD$ is comparable. Also, in many cases where the number of aligned positions is larger or comparable to the other methods, our learning method is able to achieve a smaller ($C_\alpha$) $RMSD$ than the other methods tested.

*Keywords:* protein structure alignment, protein structure comparison, rigid body transformation and root mean square deviation ($RMSD$)

# 1 Introduction

Protein structure alignment attempts to compare the structural similarity between protein backbone chains. A protein molecule can have one or more protein chains, and each chain consists of a series of amino acid residues connected by peptide bonds. Protein structural similarity can be used to infer evolutionary relationships, or in classifying protein structures into more generalized groups. Typically, in protein structure comparison process, each protein chain is represented by an ordered set of 3-D points where each point corresponds to an alpha-carbon ($C_\alpha$) atom in an amino acid residue. To compare the structural similarity between these "backbone" representations, a protein structure alignment algorithm seeks an optimal transformation by which chains are matched as closely as possible. An alignment is characterized by (1) how many positions are matched, (2) where these positions are and (3) how well they are matched. (1) and (2) are available once an alignment is determined. For (3), a transformation based alignment algorithm usually calculates ($C_\alpha$) $RMSD$, the root mean square distance between aligned positions.

The alignment problem is non-trivial – in fact, the problem of finding the optimal global alignment between protein structures has been shown to be NP-hard [12, 6]. Therefore, there have been a number of protein structure alignment algorithms presented in the past years (e.g. [1, 3, 4, 7, 8, 9, 11, 13, 14, 15, 16, 17, 18, 19, 21, 22, 23, 24, 25]), among them [7](Dali: distance matrix based method), [11](SSM: secondary structure matching), [16](CE: the combinatorial extension method), [21](FATCAT: protein structure alignment based on flexible transformation), are commonly used. We have developed a feedback algorithm for pairwise protein structure alignment and our web alignment tool is available for public access. Our algorithm is named SLIPSA, which stands for Self Learning and Improving Protein Structure Alignment. SLIPSA is self learning in that it has a feedback loop which sends the current alignment result back to its input in order to learn a better result in the next stage. In addition, SLIPSA accepts any reasonable upper-bound ($C_\alpha$) $RMSD$ value as one of the inputs, and outputs an alignment result with an ($C_\alpha$) $RMSD$ never greater than that value. Like CE, Dali and SSM, the SLIPSA alignment method is based on rigid body transformation, as opposed to flexible transformation-based algorithms such as the one described in [21].

Our paper is organized as follows: section 2 presents the SLIPSA algorithm; section 3 describes the framework and procedures used in SLIPSA; section 4 reports the experimental results of SLIPSA and compares it with some well known algorithms such as CE, DaliLite (the pairwise version of Dali), and SSM, each of them having a public website; section 4.3 discusses the results and concludes the paper.

# 2 SLIPSA: An Algorithm with Feedback

SLIPSA can be traced to a prototype algorithm that we reported previously in [25], but the former has proceeded far beyond the latter in terms of maturity, stability, efficiency and availability. The SLIPSA algorithm first searches all the locally similar sub-chain pairs from two protein backbone chains. Such sub-chain pairs are called local alignments. Next, consistent local alignments are grouped into global alignment candidates called "double-center stars" and a currently optimal global alignment is chosen from all the candidates. Then this output is sent back to its own input in order to learn from itself. We call this a feedback. Such feedback is repeated to obtain improved results, until finally an optimal alignment (i.e. a result with as many as possible aligned $C_\alpha$ pairs and an acceptable ($C_\alpha$) $RMSD$). SLIPSA can also learn from other algorithms when they are available.

## 2.1 General Algorithmic Concepts

As shown in Figure 1, local alignments are discovered by checking the distance difference between corresponding $C_\alpha$ pairs. A local alignment $L = (i, j, l)$ is defined as the longest consecutive stretch of $C_\alpha$ pairs starting from position $i$ in protein backbone chain $S = p_1 \cdots p_n$ and position $j$ in backbone chain $S' = q_1 \cdots q_m$ and having length $l$, such that $|d(p_{i+u}, p_{i+v}) - d(q_{j+u}, q_{j+v})| \leq 2\epsilon$ for any $0 \leq u, v \leq l-1$ and $u \neq v$, where $d(p, q)$ is the Euclidean distance between two 3-D points $p$ and $q$, and $\epsilon$ is a small constant. A local alignment has to be long enough to make sense.

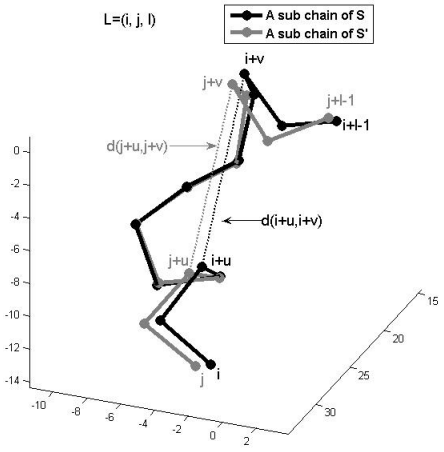


Figure 1: Local alignment L=$(i, j, l)$

After local alignments are discovered, they are organized into groups. Ideally, only consistent local alignments should be added to the same group. Suppose there are two local alignments $L_1 = (i_1, j_1, l_1)$ and $L_2 = (i_2, j_2, l_2)$, the point set $P = \{p_{i_1}, \cdots, p_{i_1+l_1-1}, p_{i_2}, \cdots, p_{i_2+l_2-1}\}$ is all the aligned points in the first chain, including those in $L_1$ and $L_2$, and $Q = \{q_{j_1}, \cdots, q_{j_1+l_1-1}, q_{j_2}, \cdots, q_{j_2+l_2-1}\}$ is all the aligned points in the second chain, also including those in $L_1$ and $L_2$. We say that local alignments $L_1$ and $L_2$ are consistent if, after applying a rigid body transformation to $Q$, the $(C_\alpha)$ $RMSD$ between $P$ and transformed $Q$ is small enough. In other words, if we have a set of local alignments, we conclude that all these local alignments are consistent if all the local alignments share a common rigid body transformation which makes them consistent with each other. Therefore a global alignment can be defined as such a set of consistent local alignments with a common transformation and an acceptable $(C_\alpha)$ $RMSD$.

The consistency relationship between local alignments can be represented as a graph. Given $A_L = \{L_1, L_2, \cdots, L_w\}$ where each $L_u = (i_u, j_u, l_u)$ $(1 \leq u \leq w)$ is a local alignment. A graph $G = (V, E)$ is defined accordingly, where each local alignment is a vertex of the graph, $V = A_L$ is the vertex set and $E$ is the edge set. Edge $e_{uv}, e_{vu} \in E$ if and only if $L_u$ and $L_v$ are consistent. With this representation, grouping mutually consistent local alignments is equivalent to finding cliques in a graph, which is an NP-complete problem. A possible simplification to this problem is to look for "stars" rather than cliques in a graph. A star is a set of vertices including a center and all the other vertices that are connected to the center vertex. Since any clique must be included in some star, for our particular problem this simplification will not miss useful vertices. Figure 2 shows a graph, two cliques and an example star. There are 6 stars in the graph since $|V|$=6. They are $Star_1 = Star_2 = Star_6 = \{L_1, L_2, L_5, L_6\}$, $Star_3 = Star_4 = \{L_3, L_4, L_5\}$ and $Star_5 = \{L_1, L_2, L_3, L_4, L_5, L_6\}$. A set of all the unique stars is $Stars = \{Star_1, Star_3, Star_5\}$. Note that each star is finally a set of local alignments and each local alignment is a set of $C_\alpha$ pairs.

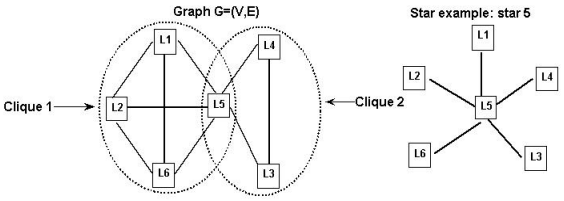


Figure 2: An example star

For each unique star, a corresponding global alignment candidate is calculated by deleting badly aligned $C_\alpha$ pairs involved in that star. Then all the candidates are compared and the optimal one is chosen. An example global alignment between protein chains 1ATP:E and 1PHK is shown in Figure 3, where $N_{mat}$ is the number of aligned $C_\alpha$ pairs, $(C_\alpha)$ $RMSD$ is the root mean square distance between the aligned pairs, and the rigid body transformation used to align the two chains is $T$ (the translation vector) and $R$ (the rotation matrix).

The "star" approach has been used in the earlier version of this algorithm [25], which has one center for each of its stars and shows some instability for aligning large proteins. We introduce the double-center method to group the local alignments and it is described

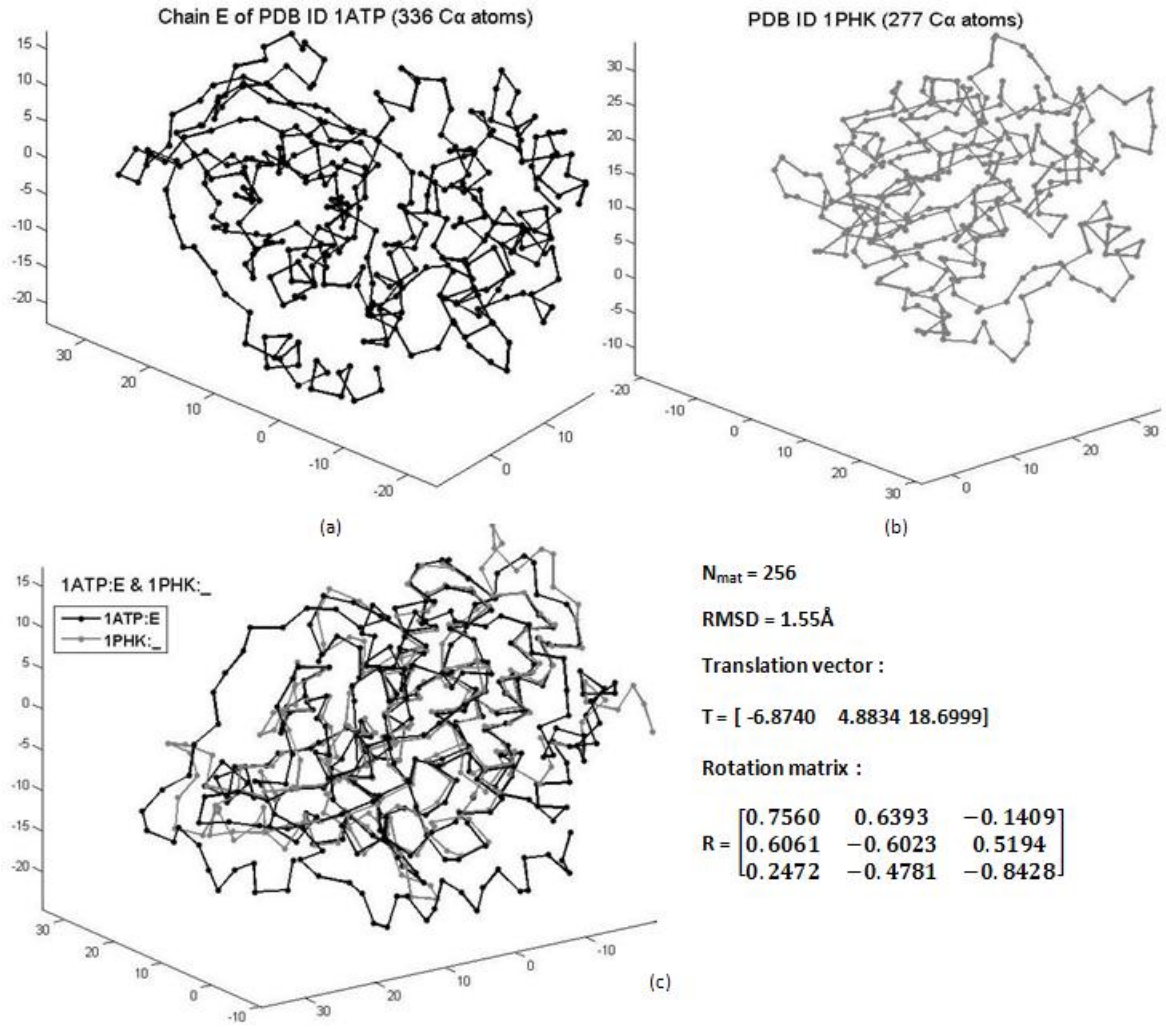


Figure 3: A global alignment

in section 2.2. This greatly improves the reliability of the algorithm. Another crucial new technical development of this paper is the learning strategy based on feedback, which is described in section 2.3. The combination of two new methods greatly improves speed, reliability, and accuracy of the algorithm.

## 2.2 Introduction of Double-center "Stars"

The single-center star method is not flawless. It works well when the two protein chains match well or the chain diameters are small. However, we have found that it is less stable when the chains do not match very well or the chain diameters are large. This is caused by deleting badly matched $C_\alpha$ pairs from each star, a method applied to obtain a global alignment candidate. When local alignments are grouped into an initial star, there may exist point pairs which do not match well. An initial transformation is calculated and the worst matched pair based on that transformation is first deleted, then the transformation

is recalculated to select the second worst pair. This process is repeated. In this way the well matched pairs survive and the $(C_\alpha)$ $RMSD$ becomes smaller and smaller, until an acceptable $(C_\alpha)$ $RMSD$ is achieved. The effect of deleting bad point pairs relies on a good initial transformation, which in turn depends on the star center selection. With a single star center, the initial transformation has great freedom to move and rotate in the point pair deletion process, thus the deletion may go along a more unpredictable way. This is more obvious when the local alignments are relatively short, which usually happens when the chains do not match very well or the chain diameters are large. Based on this observation, we consider grouping local alignments into double-center "stars".

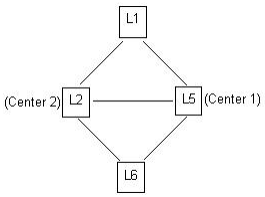


Figure 4: A double-center star

A "double-center star" is, as suggested by its name, a "star" with two centers. Each single-center star can be extended to a corresponding double-center star, while the latter is much more stable. In a single-center star, each local alignment consistent with the center is added to the star, while in a double-center star, a local alignment can be added only when it is consistent with both centers. The first center of a double-center star is exactly the one in a single-center star, and the second center is selected from that star. The selection of the second center satisfies the following conditions: (1) It is consistent with the first center; (2) It is long enough to make sense; (3) It is as far as possible from the first center. Figure 4 illustrates a double-center star corresponding to star 5 in Figure 2, suppose $L_2$ is the second center.

Each local alignment in a single-center star is consistent with the center, however, this does not automatically guarantee that all the local alignments in the star are consistent. The consistency relationship is not necessarily transitive. To reduce the probability of adding inconsistent local alignments to the star, a double-center star accepts local alignments in a more prudent way. It rejects the local alignments originally surviving in the single-center star on a weak basis, therefore local alignments in the double-center star are more likely to be those very good ones. To some extent, the presence of the second center has the effect of "extending" the local alignment in the first center. With such a long "local alignment" as the center, the star will be more stable because points in it have much less freedom to move or rotate. From another aspect, with this improvement the extent to which the initial transformation will change along with the deletion of bad point pairs is reduced significantly - the initial transformation will be closer to the final one, and thus the deletion will cause less unpredictability. Furthermore, the filtering of unpromising local alignments reduces their negative contribution to the overall transformation (as well as the number of point pairs involved in the initial star), speeding up the deletion process and resulting in a faster and better global alignment.

## 2.3 Development of Learning Ability

### 2.3.1 Self-learning

As we have mentioned, good star centers produce promising stars and have a greater probability of generating good global alignments. However, thus far the selection of star centers has been naïve: any local alignment with sufficient length can be the center of a star. The

double-center method helps remove some unpromising local alignments from a star when the first center is determined, but it contributes nothing to the selection of the first center. If the first center of a star can be selected intelligently rather than by arbitrarily picking up a local alignment, then the star may yield a better global alignment. This intelligence may be difficult to achieve without any a priori knowledge on the global structural similarity between the two chains. However, when such knowledge is available, it is possible to improve the alignment by way of a self-learning strategy.

Once a currently optimal global alignment is output, we are able to know approximately where the aligned positions are. We organize the consecutively aligned point pairs into groups, and each group of consecutive point pairs is called a global alignment segment. A global alignment segment looks exactly like a local alignment, while as a part of a good global alignment, it should be a good "local alignment". Here local alignment is quoted because global alignment segments are not output of the local alignment phase, although there is no substantial difference between both definitions. To take advantage of these good global alignment segments, we apply a feedback mechanism to teach our alignment algorithm how to improve itself. The self-learning is implemented via the iterative utilization of its own output. When a global alignment is ready, consecutive alignment segments are extracted, then each segment is used as a new star center and local alignments consistent with the center are added to its group. This global alignment phase is repeated with a few new stars obtained from the currently optimal global alignment, until the alignment output converges (i.e. no changes are found between two iterations).

### 2.3.2 Learning from others

When a global alignment from another algorithm is available, the global alignment segments in that result can work as initial star centers. These centers are likely to be better than our own local alignments because they are from an optimal alignment result obtained from another algorithm. With these centers, our global alignment searching starts from a very good jumping-off point, therefore it is possible to output a result better than without learning. Learning from other algorithms may be more effective in the cases our algorithm performs worse than others. When it performs better than other algorithms even without learning, this learning may be less necessary, however it is never harmful, because if it results in a worse global alignment, its results can simply be disregarded. Therefore the combination of self-learning and learning-from-others will never output an alignment worse than the one of another algorithm. In the worst case it outputs nothing different. For this reason, our algorithm can also be used to improve the result of any other algorithm. We call this a refinement to that algorithm.

# 3 The Formal Description of SLIPSA

We give the formal description of SLIPSA. Combining the double-center star, the self-learning and the learning-from-others methods which use feedback, we greatly improve our earlier work [25] and have found interesting results when comparing SLIPSA with some other algorithms. The SLIPSA framework is shown in Figure 5. This system takes six parameters:

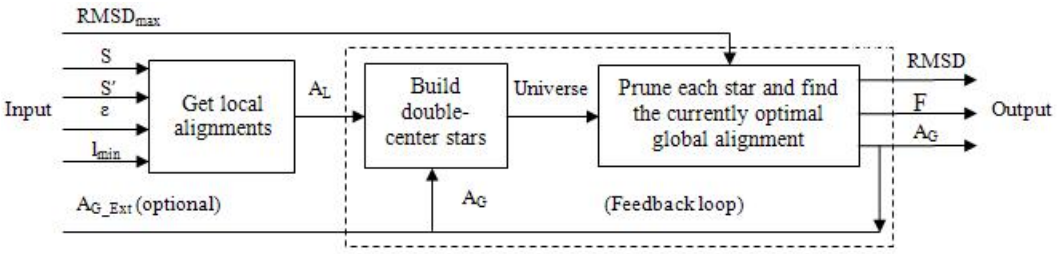


Figure 5: The SLIPSA framework

protein chains $S$ and $S'$, $RMSD_{max}$ (a user specified maximum $(C_\alpha)$ $RMSD$), distance constant $\epsilon$, minimum local alignment length $l_{min}$, and an optional external global alignment $A_{G\_Ext}$. Parameters $S$ and $S'$ are determined by the user, $RMSD_{max}$ is either determined by the user or obtained from another algorithm, $\epsilon$ and $l_{min}$ are selected empirically according to the user input, and $A_{G\_Ext}$ is either empty or also obtained from the external algorithm. The system outputs an optimal global alignment result consisting of $A_G$ (a set of global alignment segments), $(C_\alpha)$ $RMSD$ (a value not greater than $RMSD_{max}$) and $F$ (a rigid body transformation corresponding to the final global alignment). The following sub-sections describe the details of the SLIPSA algorithm.

## 3.1 Getting Local Alignments

The calculation of local alignments has been reviewed in section 2.1. The procedure used to get local alignments can be from either [25] or other related papers (e.g. [21]). The procedure body is omitted.

**Get-Local-Alignments**$(S, S', \epsilon, l_{\min})$

Input: protein backbone chains $S = p_1 \cdots p_n$, $S' = q_1 \cdots q_m$, distance constant $\epsilon$ and minimum local alignment length $l_{\min}$, where each $p_i$ or $q_i$ is a 3-D point corresponding to a $C_\alpha$ atom in a protein backbone.

Output: $A_L = \{L_1, L_2, \cdots, L_w\}$, a set containing all the local alignments of length $\geq l_{\min}$ between $S$ and $S'$.

## 3.2 Building up Stars from Local Alignments

The improved procedure outputs double-center stars. The input is star centers from a set of global alignment segments, or from a local alignment set when the former is empty. The non-center nodes in a star are still chosen from the local alignment set.

**Build-Double-Center-Stars**$(A_L, A_G)$

Input: $A_L = \{L_1, L_2, \cdots, L_w\}$ and $A_G = \{L_{1'}, L_{2'}, \cdots, L_{w'}\}$, where $A_L$ is a set of local alignments and $A_G$ is a set of global alignment segments.

Output: $Universe = \{Star_1, Star_2, \cdots, Star_k\}$, a set of all the unique double-center stars.

**begin**

$Universe \leftarrow \{\}$ (the empty set);

**if** $(A_G = \{\})$ **then** $A \leftarrow A_L$; **otherwise** $A \leftarrow A_G$;

**for** (each local alignment $L_u$ in $A$)
find $L_{u'}$, the second center based on $L_u$, in $A$;
$Star_u \leftarrow \{L_u, L_{u'}\}$;
**for** (each local alignment $L_v$ in $A_L$)
**if** ($L_v$ is consistent with both $L_u$ and $L_{u'}$) **then** $Star_u \leftarrow Star_u \cup \{L_v\}$;
**end for**
**if** ($Star_u \notin Universe$) **then** $Universe \leftarrow Universe \cup \{Star_u\}$;
**end for**
**return** $Universe$;
**end**

## 3.3 Finding a Global Alignment from the Stars

In each iteration of our algorithm, a global alignment is output and used as an input of the next iteration. We describe how to prune the set of aligned pairs in a star and obtain the global alignment which has an ($C_\alpha$) $RMSD$ not greater than that specified by the user. We refine a similar idea that is used in our another algorithm [25], which does not use feedback.

**Prune-One-Star(**$Star, RMSD_{max}$**)**
Input: a $Star$ and $RMSD_{max}$ (a user specified maximum $RMSD$).
Output: $(A_S, RMSD_S, F_S, l_S)$, where $A_S = \{L_{1''}, L_{2''}, \cdots, L_{w''}\}$ is a set of global alignment segments which share a common transformation $F_S$ with $RMSD_S \leq RMSD_{max}$, and $l_S$ is the number of aligned point pairs in $A_S$.
**begin**
$A_S \leftarrow Star$;
$l_S \leftarrow$ the number of point pairs involved in $A_S$;
calculate transformation $F_S$ and $RMSD_S$ for all the point pairs involved in $A_S$;
**while** ($RMSD_S > RMSD_{max}$)
delete point pair $(p, q)$ with the largest $d(p, F_S(q))$ in $A_S$;
$l_S \leftarrow l_S - 1$;
recalculate transformation $F_S$ and $RMSD_S$ for all the point pairs involved in $A_S$;
**end while**
**return** $(A_S, RMSD_S, F_S, l_S)$;
**end**

In the following function Find-Global-Alignment(), we apply the Prune-One-Star() procedure to each of the stars in the universe which is built from Build-Double-Center-Stars(). The alignment that contains the largest number of aligned pairs will be returned.

**Find-Global-Alignment(**$Universe, RMSD_{max}$**)**
Input: $Universe = \{Star_1, Star_2, \cdots, Star_k\}$ and $RMSD_{max}$ (a user specified maximum $RMSD$).
Output: $(A_G, RMSD, F)$, where $A_G = \{L_{1'}, L_{2'}, \cdots, L_{w'}\}$ is a set of global alignment segments which share a common transformation $F$ with $RMSD \leq RMSD_{max}$.
**begin**
sort $Universe$ by a descending order of the number of 3-D point pairs involved in each star;
$l_{max} \leftarrow 0$;

**for** (each $Star_u$ in $Universe$)
$(A_S, RMSD_S, F_S, l_S) \leftarrow$ Prune-One-Star($star_u, RMSD_{max}$);
**if** ($l_S > l_{max}$) **then** $A_G \leftarrow A_S$; $RMSD \leftarrow RMSD_S$; $F \leftarrow F_S$; $l_{max} \leftarrow l_S$;
**end for**
**return** $(A_G, RMSD, F)$;
**end**

### 3.4 The Feedback Procedure

This is the main procedure of SLIPSA. It calls Get-Local-Alignments in the first step, then Build-Double-Center-Stars and Find-Global-Alignment are called repeatedly. A global alignment output by the current iteration serves as the input of the next iteration. The procedure terminates when the global alignment ceases to change (i.e. converges).
SLIPSA($S, S', \epsilon, l_{min}, RMSD_{max}, A_{G\_Ext}$)
Input: $S, S', \epsilon, l_{min}$, $RMSD_{max}$ and $A_{G\_Ext}$, where $A_{G\_Ext}$ can be either empty or a set of global alignment segments obtained from an external algorithm.
Output: $(A_G, RMSD, F)$.
**begin**
$A_L \leftarrow$ Get-Local-Alignments($S, S', \epsilon, l_{min}$);
$A_G \leftarrow A_{G\_Ext}$;
**do**
$A'_G \leftarrow A_G$;
$Universe \leftarrow$ Build-Double-Center-Stars($A_L, A'_G$);
$(A_G, RMSD, F) \leftarrow$ Find-Global-Alignment($Universe, RMSD_{max}$);
**while** ($A_G \neq A'_G$);
**return** $(A_G, RMSD, F)$;
**end**

When no external alignment is available, procedure SLIPSA is called by way of SLIPSA($S$, $S'$, $\epsilon$, $l_{min}$, $RMSD_{max}$, {}). When it is available, SLIPSA can be called as SLIPSA($S$, $S'$, $\epsilon$, $l_{min}$, $RMSD_{max}$, $A_{G\_Ext}$). We call this a refinement to external alignment $A_{G\_Ext}$. To independently test the performance of our algorithm, none of the experiments reported in section 4 uses any external alignment as our input.

## 4 Experimental Environment and Results

### 4.1 Our Web Alignment Tool

We have developed a web alignment tool based on the SLIPSA algorithm. The website is available for public access at http://fpsa.cs.uno.edu/. It is not only a SLIPSA alignment tool but also an alignment comparison tool between SLIPSA and DaliLite, CE and SSM, some commonly used protein structure alignment algorithms with public websites.

The data used for protein alignment are the PDB files downloaded from the RCSB Protein Data Bank. The files have been moved to the Worldwide Protein Data Bank (wwPDB) by

the time we wrote this paper. As of January 2008, there were over 48,000 protein structures with over 90,000 chains discovered.

Our website is built on an Intel dual-Xeon 3G Hz PC server with 3GB memory. The web development tools we have used include Apache HTTP server with PHP support, ActivePerl and MySQL database server. The SLIPSA algorithm is written in MATLAB. See [20] and [2] for the rigid body transformation method that we have used in SLIPSA.

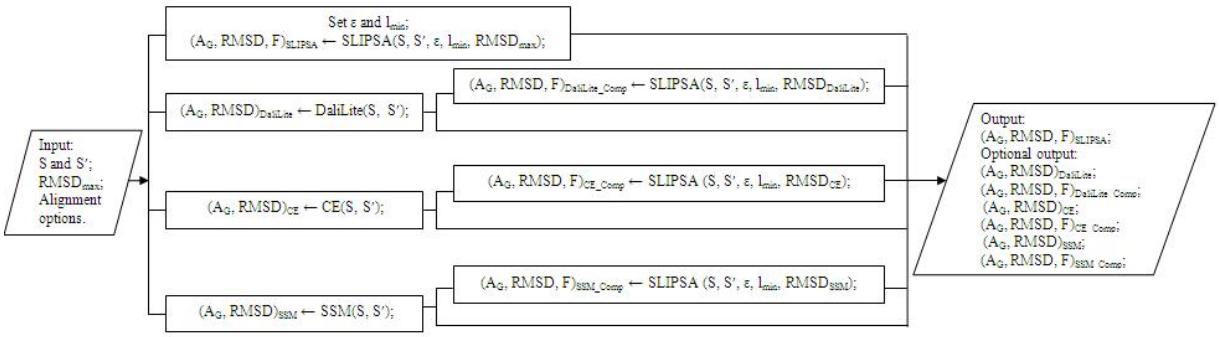


Figure 6: The web alignment work flow

The work flow of our website is shown in Figure 6. Besides a maximum value for $(C_\alpha)$ $RMSD$, it accepts either PDB IDs or user uploaded PDB files as input. It is optional to compare SLIPSA with DaliLite, CE or SSM. When a comparing option is chosen, our tool automatically submits alignment request to and retrieves result from DaliLite, CE or SSM website, and performs SLIPSA alignment according to the retrieved $(C_\alpha)$ $RMSD$ value. The website outputs the following alignment results. Beyond the first result listed, all others are optional depending on the user choices. Note that SLIPSA outputs $A_G$ (a set of global alignment segments), $(C_\alpha)$ $RMSD$ and $F$ (a rigid body transformation).

(1) $(A_G, RMSD, F)_{\text{SLIPSA}}$: the SLIPSA result with a user specified $RMSD_{max}$.

(2) $(A_G, RMSD)_{DaliLite}$: the DaliLite result retrieved automatically from its website.

(3) $(A_G, RMSD, F)_{DaliLite\_Comp}$: the SLIPSA result with an $RMSD$ retrieved from DaliLite website as input. This result is used to compare SLIPSA with DaliLite.

(4) $(A_G, RMSD)_{CE}$: the CE result retrieved automatically from its website.

(5) $(A_G, RMSD, F)_{CE\_Comp}$: the result used to compare SLIPSA with CE.

(6) $(A_G, RMSD)_{SSM}$: the SSM result retrieved automatically from its website.

(7) $(A_G, RMSD, F)_{SSM\_Comp}$: the result used to compare SLIPSA with SSM.

## 4.2 Experimental Results

We have collected 224 alignment cases to test the performance of our algorithm. The test cases were originally proposed by various papers for various testing purposes. Table 1 lists all the 224 cases. They include No. 1 - No. 20 (see Table III in [16]), No. 21 - No. 88 (see Table I in [5]), No. 89 (see Tables I and II in [16]), No. 90 - No. 92 (supplement to Table III in [16]), No. 93 (see Figure 5 in [16]), No. 94 - No. 101 (see Table IV in [16]), No. 102 - No. 111 (see Table V in [16]), No. 112 - No. 120 (supplement to Table V in [16]), No. 121 - No. 124 (see Table VII in [16]), No. 125 - No. 143 (see Table 1 in [15]), No. 144 - No. 183 (see Table 1 in [22]) and No. 184 - No. 224 (see Table 2 in [22]).

Table 1: PDB chains of the 224 test cases

| No. | Chain 1 | Chain 2 | No. | Chain 1 | Chain 2 | No. | Chain 1 | Chain 2 | No. | Chain 1 | Chain 2 |
|---|---|---|---|---|---|---|---|---|---|---|---|
| 1 | 1ATP:E | 1APM:E | 57 | 2AK3:A | 1GKY:_ | 113 | 1HLE:B | 2ACH:B | 169 | 1MBC:_ | 1PHN:A |
| 2 | 1ATP:E | 1CDK:A | 58 | 1ATN:A | 1ATR:_ | 114 | 1BBT:4 | 1TMF:4 | 170 | 1MBC:_ | 1CPC:A |
| 3 | 1ATP:E | 1YDR:E | 59 | 1ARB:_ | 5PTP:_ | 115 | 1AIE:_ | 2FUA:_ | 171 | 1MBC:_ | 1LIA:A |
| 4 | 1ATP:E | 1CTP:E | 60 | 2PIA:_ | 1FNB:_ | 116 | 1CPT:_ | 1FCT:_ | 172 | 1MBC:_ | 1CPC:B |
| 5 | 1ATP:E | 1PHK:_ | 61 | 3RUB:L | 6XIA:_ | 117 | 1LBD:_ | 1PSM:_ | 173 | 1MBC:_ | 1QGW:C |
| 6 | 1ATP:E | 1KOA:_ | 62 | 2SAR:A | 9RNT:_ | 118 | 4ICB:_ | 1CTD:A | 174 | 1MBC:_ | 1LIA:B |
| 7 | 1ATP:E | 1KOB:A | 63 | 3CD4:_ | 2RHE:_ | 119 | 2SEC:I | 1EGP:A | 175 | 1MBC:_ | 1COL:A |
| 8 | 1ATP:E | 1AD5:A | 64 | 1AEP:_ | 256B:A | 120 | 1SCE:A | 1PUC:_ | 176 | 1MBC:_ | 2CP4:_ |
| 9 | 1ATP:E | 1CKI:A | 65 | 2MNR:_ | 4ENL:_ | 121 | 1BPI:_ | 1BUN:B | 177 | 1MBC:_ | 1EUM:A |
| 10 | 1ATP:E | 1CSN:_ | 66 | 1LTS:D | 1BOV:A | 122 | 1BPI:_ | 5EBX:_ | 178 | 1MBC:_ | 1FPO:A |
| 11 | 1ATP:E | 1ERK:_ | 67 | 2GBP:_ | 2LIV:_ | 123 | 1WAJ:_ | 1NOY:A | 179 | 1MBC:_ | 1OXA:_ |
| 12 | 1ATP:E | 1FIN:A | 68 | 1BBT:1 | 2PLV:1 | 124 | 1WAJ:_ | 1XWL:_ | 180 | 1MBC:_ | 1LE2:_ |
| 13 | 1ATP:E | 1GOL:_ | 69 | 2MTA:C | 1YCC:_ | 125 | 1ACX:_ | 1COB:B | 181 | 1MBC:_ | 2FHA:_ |
| 14 | 1ATP:E | 1JST:A | 70 | 1TAH:A | 1TCA:_ | 126 | 1ACX:_ | 1TMF:A | 182 | 1MBC:_ | 1NFN:_ |
| 15 | 1ATP:E | 1IRK:_ | 71 | 1RCB:_ | 2GMF:A | 127 | 1PTS:A | 1MUP:_ | 183 | 1MBC:_ | 1GRJ:_ |
| 16 | 1ATP:E | 1FGK:A | 72 | 1SAC:A | 2AYH:_ | 128 | 2GBL:_ | 1UBQ:_ | 184 | 3TRX:_ | 4TRX:_ |
| 17 | 1ATP:E | 1FMK:_ | 73 | 1DSB:A | 2TRX:A | 129 | 2GB1:_ | 4FXC:_ | 185 | 3TRX:_ | 1MDI:A |
| 18 | 1ATP:E | 1WFC:_ | 74 | 1STF:I | 1MOL:A | 130 | 1UBQ:_ | 4FXC:_ | 186 | 3TRX:_ | 1AIU:_ |
| 19 | 1ATP:E | 1KNY:A | 75 | 2AFN:A | 1AOZ:A | 131 | 1PLC:_ | 2RHE:_ | 187 | 3TRX:_ | 1ERV:_ |
| 20 | 1ATP:E | 1TIG:_ | 76 | 1FXI:A | 1UBQ:_ | 132 | 1PLC:_ | 1ACX:_ | 188 | 3TRX:_ | 1F9M:B |
| 21 | 1MDC:_ | 1IFC:_ | 77 | 1BGE:B | 2GMF:A | 133 | 1ACX:_ | 1RBE:_ | 189 | 3TRX:_ | 1F9M:A |
| 22 | 1NPX:_ | 3GRS:_ | 78 | 3HLA:B | 2RHE:_ | 134 | 1ABA:_ | 1TRS:_ | 190 | 3TRX:_ | 1GH2:A |
| 23 | 1ONC:_ | 7RSA:_ | 79 | 3CHY:_ | 2FOX:_ | 135 | 1ABA:_ | 1DSB:A | 191 | 3TRX:_ | 1EP7:A |
| 24 | 1OSA:_ | 4CPV:_ | 80 | 2AZA:A | 1PAZ:_ | 136 | 1ABA:_ | 1PBF:_ | 192 | 3TRX:_ | 1EP7:B |
| 25 | 1PFC:_ | 3HLA:B | 81 | 1CEW:I | 1MOL:A | 137 | 1MJC:_ | 5TSS:A | 193 | 3TRX:_ | 1FAA:A |
| 26 | 2CMD:_ | 6LDH:_ | 82 | 1CID:_ | 2RHE:_ | 138 | 1PGB:_ | 5TSS:A | 194 | 3TRX:_ | 1TOF:_ |
| 27 | 2PNA:_ | 1SHA:A | 83 | 1CRL:_ | 1EDE:_ | 139 | 2TMV:P | 256B:A | 195 | 3TRX:_ | 2TIR:_ |
| 28 | 1BBH:A | 2CCY:A | 84 | 2SIM:_ | 1NSB:A | 140 | 1TNF:A | 1BMV:1 | 196 | 3TRX:_ | 1THX:_ |
| 29 | 1C2R:A | 1YCC:_ | 85 | 1TEN:_ | 3HHR:B | 141 | 1UBQ:_ | 1FRD:_ | 197 | 3TRX:_ | 1FB6:B |
| 30 | 1CHR:A | 2MNR:_ | 86 | 1TIE:_ | 4FGF:_ | 142 | 2RSL:C | 3CHY:_ | 198 | 3TRX:_ | 1QUW:A |
| 31 | 1DXT:B | 1HBG:_ | 87 | 2SNV:_ | 5PTP:_ | 143 | 3CHY:_ | 1RCF:_ | 199 | 3TRX:_ | 1KTE:_ |
| 32 | 2FBJ:L | 8FAB:B | 88 | 1GPL:_ | 2TRX:A | 144 | 1MBC:_ | 5MBN:_ | 200 | 3TRX:_ | 1JHB:_ |
| 33 | 1GKY:_ | 3ADK:_ | 89 | 1CPC:L | 1COL:A | 145 | 1MBC:_ | 1MBN:_ | 201 | 3TRX:_ | 3GRX:_ |
| 34 | 1HIP:_ | 2HIP:A | 90 | 1KNY:A | 1TIG:_ | 146 | 1MBC:_ | 1MYH:A | 202 | 3TRX:_ | 1H75:A |
| 35 | 2SAS:_ | 2SCP:A | 91 | 1MAE:H | 2BBK:J | 147 | 1MBC:_ | 1HDS:B | 203 | 3TRX:_ | 1EGO:_ |
| 36 | 1FCL:A | 2FB4:H | 92 | 2MHR:_ | 2BRD:_ | 148 | 1MBC:_ | 2DHB:A | 204 | 3TRX:_ | 1ILO:A |
| 37 | 2HPD:A | 2CPP:_ | 93 | 1HCL:_ | 1JSU:A | 149 | 1MBC:_ | 1MBA:_ | 205 | 3TRX:_ | 1ABA:_ |
| 38 | 1ABA:_ | 1EGO:_ | 94 | 2ASR:_ | 1OCC:C | 150 | 1MBC:_ | 1DM1:A | 206 | 3TRX:_ | 1FO5:A |
| 39 | 1EAF:_ | 4CLA:_ | 95 | 2ASR:_ | 1MMO:D | 151 | 1MBC:_ | 1HLM:_ | 207 | 3TRX:_ | 1MEK:_ |
| 40 | 2SGA:_ | 5PTP:_ | 96 | 2ASR:_ | 2BRD:_ | 152 | 1MBC:_ | 2LHB:_ | 208 | 3TRX:_ | 1A8Y:_ |
| 41 | 2HHM:A | 1FBP:A | 97 | 256B:A | 1AEP:_ | 153 | 1MBC:_ | 2FAL:_ | 209 | 3TRX:_ | 1E2Y:A |
| 42 | 1AAJ:_ | 1PAZ:_ | 98 | 256B:A | 1CIY:_ | 154 | 1MBC:_ | 1HBG:_ | 210 | 3TRX:_ | 1E2Y:C |
| 43 | 5FD1:_ | 1IQZ:A | 99 | 256B:A | 1AGS:A | 155 | 1MBC:_ | 1ITH:A | 211 | 3TRX:_ | 1QMV:A |
| 44 | 1ISU:A | 2HIP:A | 100 | 2ASR:_ | 1LKI:_ | 156 | 1MBC:_ | 1FLP:_ | 212 | 3TRX:_ | 1BJX:_ |
| 45 | 1GAL:_ | 3COX:_ | 101 | 2ASR:_ | 1FPS:_ | 157 | 1MBC:_ | 1ECA:_ | 213 | 3TRX:_ | 1GP1:B |
| 46 | 1CAU:B | 1CAU:A | 102 | 1LIS:_ | 1CIY:_ | 158 | 1MBC:_ | 2HBG:_ | 214 | 3TRX:_ | 1QQ2:A |
| 47 | 1HOM:_ | 1LFB:_ | 103 | 1CFP:A | 4ICB:_ | 159 | 1MBC:_ | 1ASH:_ | 215 | 3TRX:_ | 1EZK:A |
| 48 | 1TLK:_ | 2RHE:_ | 104 | 1RPA:_ | 1HIW:A | 160 | 1MBC:_ | 1HBI:B | 216 | 3TRX:_ | 1EWX:A |
| 49 | 2OMF:_ | 2POR:_ | 105 | 1HYP:_ | 1MZM:_ | 161 | 1MBC:_ | 1GDI:_ | 217 | 3TRX:_ | 1QK8:A |
| 50 | 1LGA:A | 2CYP:_ | 106 | 1CLC:_ | 1HOE:_ | 162 | 1MBC:_ | 1HLB:_ | 218 | 3TRX:_ | 1FG4:A |
| 51 | 1MIO:C | 2MIN:B | 107 | 1UTG:_ | 1NOX:_ | 163 | 1MBC:_ | 1LH2:_ | 219 | 3TRX:_ | 1A8L:_ |
| 52 | 4SBV:A | 2TBV:A | 108 | 1FAR:_ | 1PTQ:_ | 164 | 1MBC:_ | 1H97:A | 220 | 3TRX:_ | 1FG4:B |
| 53 | 8I1B:_ | 4FGF:_ | 109 | 1KUM:_ | 1TUL:_ | 165 | 1MBC:_ | 1DLY:A | 221 | 3TRX:_ | 1FVK:A |
| 54 | 1HRH:A | 1RNH:_ | 110 | 1PYI:A | 1PYC:_ | 166 | 1MBC:_ | 1IDR:A | 222 | 3TRX:_ | 1F37:A |
| 55 | 1MUP:_ | 1RBP:_ | 111 | 1VIH:_ | 1PYT:A | 167 | 1MBC:_ | 1DLW:A | 223 | 3TRX:_ | 1F37:B |
| 56 | 1CPC:L | 1COL:A | 112 | 1LYP:_ | 1OLG:A | 168 | 1MBC:_ | 1ALL:A | 224 | 3TRX:_ | 1GHH:A |

Based on this test set, we compare SLIPSA with DaliLite, CE and SSM in terms of $N_{mat}$ (the number of aligned positions) and ($C_\alpha$) $RMSD$. The detailed results are listed in the appendix. In each test case SLIPSA outputs an ($C_\alpha$) $RMSD$ not greater than that

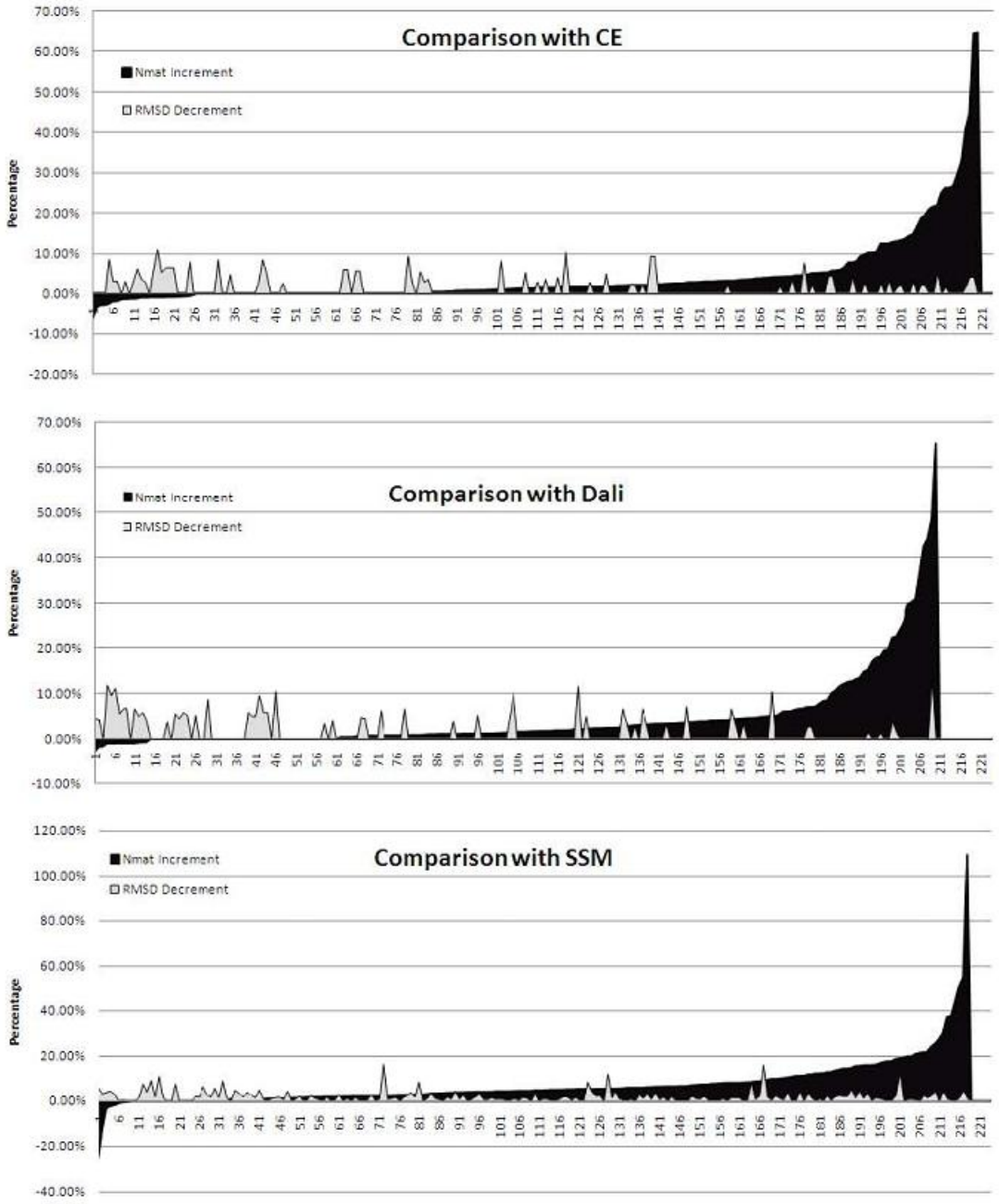


Figure 7: Comparing SLIPSA with DaliLite, CE and SSM

of DaliLite, CE, or SSM. If $N_{mat}$ of SLIPSA is larger than $N_{mat}$ of DaLiLite, CE, or SSM, we call it an $N_{mat}$ increment. Similarly, if the $(C_\alpha)$ $RMSD$ of SLIPSA is smaller than the $(C_\alpha)$ $RMSD$ of DaLiLite, CE or SSM, we call it a $(C_\alpha)$ $RMSD$ decrement. For the convenience of illustration, the results are sorted in an ascending order of the $N_{mat}$ increment rate. The $N_{mat}$ increment rate is calculated by $(N_{mat\_\text{SLIPSA}} - N_{mat\_X})$ / $N_{mat\_X}$ and the $(C_\alpha)$ $RMSD$ decrement rate is calculated by $(RMSD_X - RMSD_{\text{SLIPSA}})$ / $RMSD_X$, where $X$ is DaliLite, CE or SSM. Figure 7 illustrates such increments and decrements in percentage. It should be mentioned that (1) no SSM comparison is performed in our earlier paper [25],

(2) from the time we complete this paper, it is possible to see result changes on any of the alignment websites and we have observed minor changes on some of them, and (3) the SLIPSA experiments do not use any external alignment as input, although our algorithm is able to refine the alignment results retrieved from other web servers.

## 4.3 Discussion on the Results

Table 2 shows some statistical data based on the results in Figure 7. For each case in which an alignment result from either DaliLite, CE or SSM is missing, we were not able to compare it with SLIPSA. Also, since DaliLite, CE and SSM may have different $(C_\alpha)$ $RMSD$ values for a given test case, they are not compared mutually. Common protein alignment scoring methods such as Z-score, Q-score, P-score and geometric measures proposed in [10] all take $N_{mat}$ and $(C_\alpha)$ $RMSD$ into account. Due to the $RMSD$ flexibility of SLIPSA, it is easy to compare SLIPSA with DaliLite, CE and SSM on the basis of $N_{mat}$ because in most cases SLIPSA outputs an equal $(C_\alpha)$ $RMSD$. In our experiments, when compared with DaliLite, CE and SSM respectively, SLIPSA outputs a larger $N_{mat}$ in 66.67%, 61.82% and 86.70% of the cases; The maximum $N_{mat}$ increment rate of SLIPSA is 65.33%, 64.58% and 109.09%; Averagely, SLIPSA increases 4.56%, 4.13%, and 7.37% of the $N_{mat}$; In 26.67%, 29.09% and 81.19% of the cases SLIPSA outputs a smaller $(C_\alpha)$ $RMSD$ with the maximum $(C_\alpha)$ $RMSD$ decrement rate being 13.21%, 11.11% and 16.56%. To sum up, in most cases we see SLIPSA results with a larger or same $N_{mat}$ and a same or smaller $(C_\alpha)$ $RMSD$. In some cases that SLIPSA outputs a smaller $N_{mat}$, we also see a smaller $(C_\alpha)$ $RMSD$.

Table 2: Statistics on the experimental results

| | DaliLite | CE | SSM |
|---|---|---|---|
| Number of valid cases | 210 | 220 | 218 |
| Cases with larger $N_{mat}$ by SLIPSA | 149(66.67%) | 136(61.82%) | 189(86.70%) |
| Cases with smaller $N_{mat}$ by SLIPSA | 14(6.67%) | 26(11.82%) | 8(3.67%) |
| Maximum $N_{mat}$ increment by SLIPSA | 49 | 56 | 51 |
| Maximum $N_{mat}$ decrement by SLIPSA | 2 | 9 | 12 |
| Maximum $N_{mat}$ increment rate by SLIPSA | 65.33% | 64.58% | 109.09% |
| Maximum $N_{mat}$ decrement rate by SLIPSA | 2.74% | 6.45% | 25.53% |
| Average $N_{mat}$ increment by SLIPSA | 4.15 | 3.63 | 7.24 |
| Average $N_{mat}$ increment rate by SLIPSA | 4.56% | 4.13% | 7.37% |
| Cases with smaller $RMSD$ by SLIPSA | 56(26.67%) | 64(29.09%) | 177(81.19%) |
| Maximum $RMSD$ decrement by SLIPSA | 0.7 | 0.4 | 0.52 |
| Maximum $RMSD$ decrement rate by SLIPSA | 13.21% | 11.11% | 16.56% |
| Average $RMSD$ decrement by SLIPSA | 0.04 | 0.04 | 0.05 |
| Average $RMSD$ decrement rate by SLIPSA | 1.55% | 1.42% | 2.07% |

We also attempt to compare SLIPSA with DaliLite, CE and SSM in the cases of weak similarities. To simplify the comparison process, we tentatively define a weak similarity as a large $(C_\alpha)$ $RMSD$ between aligned chains. This definition may be incomplete, however, we have already observed some interesting results. In brief, SLIPSA obtains high average $N_{mat}$ increment rates in the weak similarity cases, and the larger the $(C_\alpha)$ $RMSD$, the higher the average $N_{mat}$ increment rate. See Table 3 for the details.

The execution time of each case by each algorithm is also recorded. A DaliLite, CE or SSM time is measured between when we submit the alignment request and when we receive the result page. The SLIPSA execution time is measured by our MATLAB program. Note that different web tools may use machines with different computation power, and different

Table 3: Comparison based on Weak Similarity

| | DaliLite | | CE | | SSM | |
|---|---|---|---|---|---|---|
| | Valid Cases | Avg. $N_{mat}$ Inc. | Valid Cases | Avg. $N_{mat}$ Inc. | Valid Cases | Avg. $N_{mat}$ Inc. |
| $RMSD \geq 5.0$ | 12 | 26.48% | 14 | 21.62% | 0 | / |
| $RMSD \geq 4.0$ | 20 | 23.48% | 41 | 14.75% | 9 | 17.50% |
| $RMSD \geq 3.0$ | 77 | 10.09% | 102 | 7.64% | 51 | 12.15% |

software implementation would result in speed changes. Therefore the time data only give a rough idea about how fast each web tool could be. The average execution time of DaliLite, CE and SSM is 16.86s, 6.14s and 9.15s, respectively. When compared with them, the average execution time of SLIPSA is 105.97s, 69.89s and 81.43s, respectively. In about 50% of the cases the SLIPSA time is below the DaliLite average, and the corresponding numbers for CE and SSM are about 25% and 28%, respectively. The speed of our algorithm is relatively slow, and occasionally we see an execution time of thousands of seconds, especially for those long chain pairs of weak similarity. It is possible to improve the speed by applying different hardware configuration and software optimization methods as well as parallel and distributed implementation.

# References


[1] L. P. Chew, K. Kedem, D. P. Huttenlocher and J. Kleinberg. Fast detection of geometric substructure in proteins. *J. of Computational Biology*, 6(3-4):313–325, 1999.

[2] D. Eggert, A. Lorusso and R. Fisher. A comparison of four algorithms for estimating 3-d rigid transformations. *British Machine Vision Conference*, 237–246, 1995.

[3] A. Falicov, and F. E. Cohen. A surface of minimum area metric for the structureal comparison of protein. *Journal of Mol. Biol.*, 258:871–892, 1996.

[4] D. Fischer, R. Nussinov and H. Wolfson. 3D substructure matching in protein molecules. *Proc. 3rd Intl Symp. Combinatorial Pattern Matching, LNCS*, 644:136–150, 1992.

[5] D. Fischer, A. Elofsson, D. Rice and D. Eisenberg. Assessing the performance of fold recognition methods by means of a comprehensive benchmark. *Proc. 1st Pacific Symposium on Biocomputing*, 300–318, 1996.

[6] A. Godzik. The structural alignment between two proteins: Is there a unique answer? *Prot. Sci.*, 5:1325–1338, 1996.

[7] L. Holm and C. Sander. Protein structure comparison by alignment of distance matrices. *J. Mol. Biol.*, 233:123–138, 1993.

[8] V. A. Ilyin, A. Abyzov and C. M.Leslin. Structural alignment of proteins by a novel TOPOFIT method, as a superimposition of common volumes at a topomax point. *Protein Science*, 13:1865–1874, 2004.

[9] R. Kolodny, N. Linial and M. Levitt. Approximate Protein Structural Alignment in Polynomial Time, *Proc. Natl. Acad. Sci. USA*, 101 (33), 12201-12206, 2004.

[10] R. Kolodny, P. Koehl and M. Levitt. Comprehensive evaluation of protein structure alignment methods: scoring by geometric measures, *J. Mol. Biol*, 346(4):1173-1188, 2005.

[11] E. Krissinel and K. Henrick. Secondary-structure matching (SSM), a new tool for fast protein structure alignment in three dimensions. *Acta Cryst.*, D60:2256–2268, 2004.

[12] R. H. Lathrop. The protein threading problem with sequence amino acid interaction preferences is NP-complete. *Protein Eng.*, 7:1059–1068, 1994.

[13] U. Lessel and D. Schomburg. Similarities between protein 3-D structures. *Protein Eng.*, 7(10):1175–87, 1994.

[14] T. Madej, J. F. Gibrat and S. H. Bryant. Threading a database of protein cores. *Proteins*, 23:356–369, 1995.

[15] A. Ortiz, C. Strauss and O. Olmea. MAMMOTH (matching molecular models obtained from theory): an automated method for model comparison. *Protein Science*, 11:2606–2021, 2002.

[16] I. N. Shindyalov and P. E. Bourne. Protein structure alignment by incremental combinatorial extension (CE) of the optimal path. *Protein Eng.*, 11:739–747, 1998.

[17] A. P. Singh and D. L. Brutlag. Hierarchical protein superposition using both secondary structure and atomic representation. *Proc. Intelligent Systems for Molecular Biology*, 284–293, 1997.

[18] W. R. Taylor and C. Orengo. Protein structure alignment. *J. Mol. Biology*, 208, 1989.

[19] W. R. Taylor. Protein structure comparison using iterated double dynamic programming. *Protein Science*, 9:654–665, 1999.

[20] S. Umeyama. Least-squares estimation of transformation parameters between two point patterns. *IEEE Tran. on Pattern Analysis and Machine Intelligence*, 13(4):376–380, 1991.

[21] Y. Ye and A. Godzik. Database searching by flexible protein structure alignment. *Protein Science*, 13(7):1841–1850, 2004.

[22] J. Ye, R. Janardan and S. Liu. Pairwise protein structure alignment based on an orientation-independent backbone representation. *Journal of Bioinformatincs and Computational Biology*, 4(2):699–717, 2005.

[23] G. Yona and K. Kedem. The URMS-RMS hybrid algorithm for fast and sensitive local protein structure alignment. *Journal of Computational Biology*, 12:12–32, 2005.

[24] Y. Zhang and J. Skolnick. TM-align: a protein structure alignment algorithm based on the TM-score. *Nucleic Acids Research*, 33:2302–2309, 2005.

[25] Z. Zhao and B. Fu. A Flexible algorithm for pairwise protein structure alignment. *the 2007 International Conference on Bioinformatics and Computational Biology*,16–22, 2007.

# Appendix

This section lists all the experimental results. In the tables, n, r and t stand for $N_{mat}$, $(C_\alpha)$ $RMSD$ and the execution time (s), respectively, $n^+$ is the $N_{mat}$ increment (%), and $r^-$ is the $(C_\alpha)$ $RMSD$ decrement (%). The results are sorted in an ascending order of $n^+$.

Table 4: Comparing SLIPSA with CE

| | CE | SLIPSA | | | CE | SLIPSA | |
|---|---|---|---|---|---|---|---|
| No. | n/r/t | n/r/t | $n^+/r^-$ | No. | n/r/t | n/r/t | $n^+/r^-$ |
| 118 | 31/1.5/3.16 | 29/1.5/0.45 | -6.45/0.00 | 119 | 33/0.6/3.13 | 33/0.6/0.55 | 0.00/0.00 |
| 17 | 256/2.8/18.97 | 247/2.8/83.78 | -3.52/0.00 | 120 | 92/1.1/3.42 | 92/1.1/1.23 | 0.00/0.00 |
| 32 | 201/2.2/4.6 | 195/2.2/16.08 | -2.99/0.00 | 121 | 55/1.5/3.27 | 55/1.5/0.34 | 0.00/0.00 |
| 41 | 237/3/10.3 | 230/3/149.39 | -2.95/0.00 | 144 | 152/0.3/3.48 | 152/0.3/1.84 | 0.00/0.00 |
| 201 | 74/2.3/3.36 | 72/2.1/8.05 | -2.70/8.70 | 145 | 152/0.5/3.41 | 152/0.5/1.42 | 0.00/0.00 |
| 215 | 97/3/3.94 | 95/2.9/20.69 | -2.06/3.33 | 146 | 153/0.6/3.46 | 153/0.6/0.44 | 0.00/0.00 |
| 216 | 97/3/3.88 | 95/2.9/22.83 | -2.06/3.33 | 148 | 141/1.6/3.57 | 141/1.5/11.92 | 0.00/6.25 |
| 109 | 64/3.5/3.66 | 63/3.5/13.64 | -1.56/0.00 | 152 | 137/1.6/3.58 | 137/1.5/11.11 | 0.00/6.25 |
| 55 | 143/3/4.73 | 141/2.9/21.44 | -1.40/3.33 | 155 | 138/1.6/3.63 | 138/1.6/21.7 | 0.00/0.00 |
| 222 | 73/2.6/3.48 | 72/2.6/9.23 | -1.37/0.00 | 156 | 137/1.7/3.52 | 137/1.6/22.44 | 0.00/5.88 |
| 203 | 75/3/3.31 | 74/2.9/7.98 | -1.33/3.33 | 157 | 136/1.7/3.52 | 136/1.6/17.16 | 0.00/5.88 |
| 38 | 77/3.1/3.39 | 76/2.9/6.95 | -1.30/6.45 | 161 | 144/2.2/3.82 | 144/2.2/19.67 | 0.00/0.00 |
| 27 | 93/2.6/3.5 | 92/2.5/10.66 | -1.08/3.85 | 164 | 141/2.2/3.86 | 141/2.2/33.03 | 0.00/0.00 |
| 220 | 96/3.2/3.74 | 95/3.1/23.77 | -1.04/3.13 | 175 | 117/3.2/4.81 | 117/3.2/101.28 | 0.00/0.00 |
| 218 | 97/3/3.83 | 96/3/21.31 | -1.03/0.00 | 184 | 105/0.4/3.23 | 105/0.4/0.33 | 0.00/0.00 |
| 197 | 102/1.6/3.3 | 101/1.5/3.86 | -0.98/6.25 | 185 | 105/0.7/3.16 | 105/0.7/0.34 | 0.00/0.00 |
| 195 | 103/1.8/3.32 | 102/1.6/6.39 | -0.97/11.11 | 186 | 105/1.3/3.27 | 105/1.3/0.69 | 0.00/0.00 |
| 196 | 103/1.8/3.33 | 102/1.7/5.63 | -0.97/5.56 | 187 | 105/1.3/3.24 | 105/1.3/0.73 | 0.00/0.00 |
| 188 | 104/1.5/3.27 | 103/1.4/2.77 | -0.96/6.67 | 190 | 105/1.5/3.3 | 105/1.5/0.84 | 0.00/0.00 |
| 189 | 104/1.5/3.19 | 103/1.4/2.66 | -0.96/6.67 | 191 | 105/1.5/3.33 | 105/1.5/2.06 | 0.00/0.00 |
| 192 | 105/1.5/3.22 | 104/1.4/3.03 | -0.95/6.67 | 193 | 104/1.6/3.3 | 104/1.6/2.84 | 0.00/0.00 |
| 54 | 117/1.9/3.63 | 116/1.9/7.09 | -0.85/0.00 | 194 | 104/1.6/3.33 | 104/1.6/2.91 | 0.00/0.00 |
| 53 | 121/2.6/3.58 | 120/2.6/10.69 | -0.83/0.00 | 198 | 101/2.1/3.35 | 101/1.9/5.78 | 0.00/9.52 |
| 93 | 266/2.3/10.42 | 264/2.3/14.64 | -0.75/0.00 | 199 | 89/3.4/3.56 | 89/3.3/22.89 | 0.00/2.94 |
| 72 | 147/3.7/7.52 | 146/3.4/45.5 | -0.68/8.11 | 212 | 96/2.4/3.44 | 96/2.4/9 | 0.00/0.00 |
| 16 | 253/3.4/15.03 | 252/3.4/67.88 | -0.40/0.00 | 213 | 100/3.5/4.45 | 100/3.3/16.06 | 0.00/5.71 |
| 1 | 336/0.3/7.2 | 336/0.3/0.84 | 0.00/0.00 | 217 | 96/3.2/3.84 | 96/3.1/21.63 | 0.00/3.13 |
| 2 | 336/0.4/7.24 | 336/0.4/0.66 | 0.00/0.00 | 223 | 73/2.6/3.33 | 73/2.5/9.94 | 0.00/3.85 |
| 3 | 336/0.5/7.22 | 336/0.5/2.73 | 0.00/0.00 | 58 | 296/3/16.52 | 297/3/254.23 | 0.34/0.00 |
| 5 | 254/1.4/7.58 | 254/1.4/18.22 | 0.00/0.00 | 50 | 261/2.4/10.41 | 262/2.4/108.42 | 0.38/0.00 |
| 21 | 128/1.9/3.64 | 128/1.9/2.84 | 0.00/0.00 | 9 | 259/2.7/14.97 | 260/2.7/73.45 | 0.39/0.00 |
| 24 | 69/2.3/4.21 | 69/2.1/8.31 | 0.00/8.70 | 15 | 257/3.7/17.84 | 258/3.7/77.91 | 0.39/0.00 |
| 25 | 96/3.3/3.55 | 96/3.3/8.75 | 0.00/0.00 | 60 | 214/2.4/10.02 | 215/2.4/120.22 | 0.47/0.00 |
| 30 | 346/1.8/6.4 | 346/1.8/93.78 | 0.00/0.00 | 45 | 415/3.2/41.37 | 417/3.2/735 | 0.48/0.00 |
| 34 | 68/2/3.28 | 68/1.9/2.05 | 0.00/5.00 | 33 | 157/3.1/5.02 | 158/3.1/122.55 | 0.64/0.00 |
| 35 | 169/3.5/4.88 | 169/3.5/47.72 | 0.00/0.00 | 40 | 154/3/5.22 | 155/3/20.72 | 0.65/0.00 |
| 57 | 157/3.5/5.44 | 157/3.5/74.16 | 0.00/0.00 | 163 | 146/2.6/4.19 | 147/2.6/15.38 | 0.68/0.00 |
| 59 | 197/3.2/7.22 | 197/3.2/89.67 | 0.00/0.00 | 149 | 141/1.8/3.67 | 142/1.8/21.33 | 0.71/0.00 |
| 63 | 91/1.8/3.48 | 91/1.8/6.41 | 0.00/0.00 | 153 | 141/1.8/3.73 | 142/1.8/23.03 | 0.71/0.00 |
| 67 | 252/4.6/16.77 | 252/4.6/836.94 | 0.00/0.00 | 159 | 138/2/3.63 | 139/2/21.97 | 0.72/0.00 |
| 75 | 249/2.5/17.41 | 249/2.5/113.05 | 0.00/0.00 | 22 | 383/2.8/25.96 | 386/2.8/396.19 | 0.78/0.00 |
| 78 | 84/3.4/3.36 | 84/3.3/18.2 | 0.00/2.94 | 14 | 252/2.4/9.55 | 254/2.4/34.19 | 0.79/0.00 |
| 81 | 81/2.3/3.69 | 81/2.1/4.14 | 0.00/8.70 | 140 | 115/4.1/5.11 | 116/4.1/36.81 | 0.87/0.00 |
| 85 | 87/1.9/3.42 | 87/1.8/5.16 | 0.00/5.26 | 167 | 111/3.1/3.8 | 112/3.1/32.97 | 0.90/0.00 |
| 86 | 116/2.9/3.72 | 116/2.9/38.28 | 0.00/0.00 | 83 | 219/3.8/25.97 | 221/3.8/418.92 | 0.91/0.00 |
| 91 | 354/0.7/6.91 | 354/0.7/21.5 | 0.00/0.00 | 79 | 108/3.6/3.71 | 109/3.3/58.25 | 0.93/8.33 |
| 102 | 93/4.5/10.42 | 93/4.5/173.11 | 0.00/0.00 | 207 | 101/2.3/3.42 | 102/2.3/8.81 | 0.99/0.00 |
| 105 | 72/3.5/3.42 | 72/3.4/23.53 | 0.00/2.86 | 26 | 280/2.2/8.5 | 283/2.2/112.55 | 1.07/0.00 |
| 106 | 65/3/5.69 | 65/3/8.5 | 0.00/0.00 | 39 | 177/2.8/5.49 | 179/2.8/31.3 | 1.13/0.00 |
| 108 | 46/1.7/3.24 | 46/1.7/0.5 | 0.00/0.00 | 12 | 252/2.2/9.58 | 255/2.2/30.3 | 1.19/0.00 |
| 110 | 38/1.3/3.3 | 38/1.3/0.72 | 0.00/0.00 | 123 | 336/1.6/43.94 | 340/1.6/186.31 | 1.19/0.00 |
| 112 | 25/0.8/3.25 | 25/0.8/0.58 | 0.00/0.00 | 42 | 80/1.8/3.42 | 81/1.7/3.75 | 1.25/5.56 |
| 113 | 30/0.9/3.18 | 30/0.9/0.8 | 0.00/0.00 | 132 | 80/3.3/3.33 | 81/3.3/6.83 | 1.25/0.00 |
| 114 | 24/1/3.18 | 24/1/1.22 | 0.00/0.00 | 206 | 79/3.3/3.4 | 80/3.3/9.02 | 1.27/0.00 |
| 115 | 24/0.6/3.17 | 24/0.6/0.81 | 0.00/0.00 | 204 | 73/3.1/3.35 | 74/3/5.41 | 1.37/3.23 |
| 117 | 32/1.6/3.48 | 32/1.6/4.25 | 0.00/0.00 | 147 | 143/1.6/3.42 | 145/1.6/10.64 | 1.40/0.00 |

Table 5: Comparing SLIPSA with CE (Continued)

| | CE | SLIPSA | | | CE | SLIPSA | |
|---|---|---|---|---|---|---|---|
| No. | n/r/t | n/r/t | $n^+/r^-$ | No. | n/r/t | n/r/t | $n^+/r^-$ |
| 202 | 71/2.6/3.32 | 72/2.5/6.78 | 1.41/3.85 | 208 | 97/2.4/4.23 | 101/2.4/13.48 | 4.12/0.00 |
| 205 | 71/2.7/3.28 | 72/2.7/10.72 | 1.41/0.00 | 171 | 119/3.5/4.59 | 124/3.5/82.08 | 4.20/0.00 |
| 150 | 141/1.9/3.77 | 143/1.9/28.14 | 1.42/0.00 | 101 | 118/5/8.89 | 123/4.9/393.2 | 4.24/2.00 |
| 66 | 68/2.3/3.39 | 69/2.2/1.17 | 1.47/4.35 | 168 | 117/3.3/4.28 | 122/3.3/72.02 | 4.27/0.00 |
| 49 | 266/3/9.83 | 270/3/224.11 | 1.50/0.00 | 211 | 92/2.1/3.63 | 96/2.1/8.45 | 4.35/0.00 |
| 160 | 133/1.9/3.66 | 135/1.7/24.03 | 1.50/10.53 | 214 | 92/2.5/3.8 | 96/2.4/12.75 | 4.35/4.00 |
| 7 | 259/2.7/14 | 263/2.7/49.09 | 1.54/0.00 | 48 | 87/1.9/3.44 | 91/1.9/3.98 | 4.60/0.00 |
| 94 | 124/2.7/4.92 | 126/2.7/69.13 | 1.61/0.00 | 173 | 130/4.9/5.06 | 136/4.9/129.34 | 4.62/0.00 |
| 18 | 244/3/14.67 | 248/3/72.45 | 1.64/0.00 | 76 | 64/3.8/3.16 | 67/3.5/3.08 | 4.69/7.89 |
| 28 | 122/1.9/3.47 | 124/1.9/10.03 | 1.64/0.00 | 183 | 62/4.4/5.52 | 65/4.4/39.23 | 4.84/0.00 |
| 43 | 61/3/3.5 | 62/3/5.75 | 1.64/0.00 | 96 | 117/4.3/6.19 | 123/4.2/126.28 | 5.13/2.33 |
| 111 | 61/3.2/3.38 | 62/3.1/8.23 | 1.64/3.13 | 99 | 97/5.4/4.64 | 102/5.4/108.45 | 5.15/0.00 |
| 137 | 61/2.7/3.58 | 62/2.7/3.5 | 1.64/0.00 | 65 | 268/3.1/12.05 | 282/3.1/336.36 | 5.22/0.00 |
| 172 | 122/3.8/4.7 | 124/3.8/104.3 | 1.64/0.00 | 4 | 302/1.5/7.66 | 318/1.5/17.58 | 5.30/0.00 |
| 165 | 112/3/3.94 | 114/3/66.5 | 1.79/0.00 | 98 | 94/4.3/9.27 | 99/4.1/99.56 | 5.32/4.65 |
| 44 | 54/1.9/3.2 | 55/1.8/1.14 | 1.85/5.26 | 219 | 86/2.2/3.81 | 91/2.1/6.39 | 5.81/4.55 |
| 46 | 159/2/4.03 | 162/2/9.19 | 1.89/0.00 | 84 | 275/3/14.53 | 291/3/317.33 | 5.82/0.00 |
| 71 | 104/4.3/3.98 | 106/4.3/58.97 | 1.92/0.00 | 169 | 117/3.5/4.05 | 124/3.5/91.53 | 5.98/0.00 |
| 47 | 50/1.1/3.33 | 51/1.1/1.84 | 2.00/0.00 | 69 | 76/2/3.72 | 81/2/7.41 | 6.58/0.00 |
| 23 | 98/2.2/3.58 | 100/2.2/5.56 | 2.04/0.00 | 130 | 64/4/3.08 | 69/4/4.64 | 7.81/0.00 |
| 29 | 97/1.9/3.48 | 99/1.9/4.09 | 2.06/0.00 | 141 | 64/4.4/3.53 | 69/4.2/4.69 | 7.81/4.55 |
| 64 | 94/4.1/3.98 | 96/4/82.73 | 2.13/2.44 | 19 | 111/4.2/10.78 | 120/4.2/256.16 | 8.11/0.00 |
| 97 | 94/4.1/3.77 | 96/4/77.3 | 2.13/2.44 | 103 | 64/2.6/3.53 | 70/2.6/7.69 | 9.38/0.00 |
| 70 | 187/2.4/10.16 | 191/2.4/50.64 | 2.14/0.00 | 104 | 71/3.2/6.46 | 78/3.1/46.8 | 9.86/3.13 |
| 125 | 92/4/3.88 | 94/3.9/20.7 | 2.17/2.50 | 200 | 78/3.2/3.47 | 86/3.2/33.42 | 10.26/0.00 |
| 209 | 92/2/3.63 | 94/2/7.86 | 2.17/0.00 | 92 | 107/4.2/5.48 | 118/4.2/77.84 | 10.28/0.00 |
| 154 | 137/2.1/3.66 | 140/1.9/22.22 | 2.19/9.52 | 36 | 48/4.3/3.3 | 53/4.3/6.88 | 10.42/0.00 |
| 158 | 137/2.1/3.68 | 140/1.9/22.11 | 2.19/9.52 | 129 | 48/3.6/3.14 | 54/3.5/3.53 | 12.50/2.78 |
| 6 | 257/2.7/16.56 | 263/2.7/62.72 | 2.33/0.00 | 142 | 80/4.1/3.34 | 90/4.1/53.98 | 12.50/0.00 |
| 80 | 84/2.9/3.5 | 86/2.9/11.05 | 2.38/0.00 | 224 | 56/5.5/3.28 | 63/5.3/18.69 | 12.50/3.64 |
| 122 | 40/5.3/3.18 | 41/5.3/1.7 | 2.50/0.00 | 177 | 62/3.8/4.89 | 70/3.8/152.3 | 12.90/0.00 |
| 8 | 236/2.5/13.73 | 242/2.5/78.69 | 2.54/0.00 | 95 | 115/5.8/12.84 | 130/5.7/653.22 | 13.04/1.72 |
| 56 | 115/3.2/5.63 | 118/3.2/97.81 | 2.61/0.00 | 178 | 75/4.4/5 | 85/4.3/105.83 | 13.33/2.27 |
| 89 | 115/3.2/5.45 | 118/3.2/97.98 | 2.61/0.00 | 176 | 88/4.3/4.89 | 100/4.3/275.34 | 13.64/0.00 |
| 166 | 114/3.8/4.16 | 117/3.8/87.33 | 2.63/0.00 | 100 | 97/5.6/5.05 | 111/5.6/160.03 | 14.43/0.00 |
| 77 | 107/3.9/4.27 | 110/3.9/131.34 | 2.80/0.00 | 107 | 54/3/3.83 | 62/2.9/17.06 | 14.81/3.33 |
| 134 | 70/2.7/3.67 | 72/2.7/8.36 | 2.86/0.00 | 138 | 48/2.9/3.41 | 56/2.9/2.88 | 16.67/0.00 |
| 151 | 140/2.1/3.83 | 144/2.1/20.91 | 2.86/0.00 | 127 | 80/4.1/3.28 | 95/4/24.56 | 18.75/2.44 |
| 162 | 139/2.3/3.55 | 143/2.3/20.81 | 2.88/0.00 | 131 | 72/5/3.17 | 86/4.9/18.23 | 19.44/2.00 |
| 31 | 133/1.8/3.72 | 137/1.8/18.14 | 3.01/0.00 | 181 | 62/3.9/5.38 | 75/3.9/126.09 | 20.97/0.00 |
| 51 | 394/3.1/40.63 | 406/3.1/652.8 | 3.05/0.00 | 179 | 88/4.5/4.95 | 107/4.5/299.27 | 21.59/0.00 |
| 87 | 130/3.1/4.16 | 134/3.1/25.64 | 3.08/0.00 | 90 | 64/7/3.34 | 78/6.6/77.94 | 21.88/5.71 |
| 82 | 97/2.9/3.8 | 100/2.9/13.55 | 3.09/0.00 | 180 | 80/6/3.81 | 100/6/390.19 | 25.00/0.00 |
| 170 | 125/4/4.48 | 129/4/83.06 | 3.20/0.00 | 88 | 80/5.4/3.8 | 101/5.3/63.84 | 26.25/1.85 |
| 10 | 248/2.4/10.42 | 256/2.4/59.03 | 3.23/0.00 | 182 | 80/6/3.75 | 101/6/303 | 26.25/0.00 |
| 174 | 124/4.2/4.66 | 128/4.1/111.48 | 3.23/2.38 | 133 | 56/7.3/3.27 | 71/7.3/23.3 | 26.79/0.00 |
| 210 | 92/2/3.54 | 95/2/10.5 | 3.26/0.00 | 20 | 54/4/6.22 | 70/4/27.47 | 29.63/0.00 |
| 37 | 366/3.4/24.1 | 378/3.4/729.19 | 3.28/0.00 | 61 | 171/3.9/35.27 | 227/3.9/863.27 | 32.75/0.00 |
| 143 | 116/3.9/4.06 | 120/3.9/103.66 | 3.45/0.00 | 221 | 64/5.3/3.41 | 90/5.2/60.84 | 40.63/1.89 |
| 13 | 253/2.6/13.14 | 262/2.6/80 | 3.56/0.00 | 135 | 56/4.5/3.25 | 81/4.3/46.39 | 44.64/4.44 |
| 62 | 84/4.5/3.48 | 87/4.5/7.31 | 3.57/0.00 | 73 | 56/4.6/3.64 | 92/4.4/36.38 | 64.29/4.35 |
| 139 | 84/3.5/3.88 | 87/3.5/31.16 | 3.57/0.00 | 136 | 48/5.2/3.64 | 79/5.2/26.2 | 64.58/0.00 |
| 52 | 156/1.9/5.36 | 162/1.9/9.64 | 3.85/0.00 | 68 | n/a | / | / |
| 74 | 78/1.7/3.28 | 81/1.7/3.3 | 3.85/0.00 | 124 | n/a | / | / |
| 11 | 253/2.6/13.2 | 263/2.6/121.42 | 3.95/0.00 | 126 | n/a | / | / |
| 116 | 25/1.3/3.54 | 26/1.3/2.63 | 4.00/0.00 | 128 | n/a | / | / |

Table 6: Comparing SLIPSA with DaliLite

| | DaliLite | SLIPSA | | | DaliLite | SLIPSA | |
|---|---|---|---|---|---|---|---|
| No. | n/r/t | n/r/t | $n^+/r^-$ | No. | n/r/t | n/r/t | $n^+/r^-$ |
| 201 | 73/2.2/14.08 | 71/2.1/6.58 | -2.74/4.55 | 194 | 105/1.7/9.2 | 105/1.7/2.06 | 0.00/0.00 |
| 44 | 58/2.3/8.44 | 57/2.2/1.22 | -1.72/4.35 | 203 | 72/2.8/14.88 | 72/2.7/7.11 | 0.00/3.57 |
| 136 | 62/3.4/13.95 | 61/3.4/15.67 | -1.61/0.00 | 207 | 102/2.3/15.04 | 102/2.3/8.77 | 0.00/0.00 |
| 197 | 102/1.7/8.75 | 101/1.5/3.98 | -0.98/11.76 | 211 | 97/2.4/9.08 | 97/2.3/9.13 | 0.00/4.17 |
| 198 | 102/2.1/19.21 | 101/1.9/5.75 | -0.98/9.52 | 219 | 91/2.1/9.95 | 91/2.1/5.98 | 0.00/0.00 |
| 195 | 103/1.8/9 | 102/1.6/6.41 | -0.97/11.11 | 14 | 261/2.9/23.14 | 262/2.9/30.56 | 0.38/0.00 |
| 196 | 103/1.8/14.03 | 102/1.7/5.59 | -0.97/5.56 | 50 | 261/2.4/19.28 | 262/2.4/112.16 | 0.38/0.00 |
| 188 | 104/1.5/8.83 | 103/1.4/2.5 | -0.96/6.67 | 16 | 246/3.1/28.06 | 247/3.1/67.97 | 0.41/0.00 |
| 189 | 104/1.5/8.82 | 103/1.4/2.58 | -0.96/6.67 | 17 | 246/2.8/31.31 | 247/2.8/85.34 | 0.41/0.00 |
| 190 | 104/1.3/8.77 | 103/1.3/0.88 | -0.96/0.00 | 3 | 334/0.5/23.08 | 336/0.5/2.69 | 0.60/0.00 |
| 192 | 105/1.5/10.24 | 104/1.4/3.03 | -0.95/6.67 | 52 | 162/2.1/13.68 | 163/2/10.44 | 0.62/4.76 |
| 28 | 125/2/8.54 | 124/1.9/11.45 | -0.80/5.00 | 151 | 144/2.2/13.61 | 145/2.1/20.67 | 0.69/4.55 |
| 155 | 139/1.7/18.55 | 138/1.6/22.63 | -0.72/5.88 | 26 | 286/2.5/28.3 | 288/2.5/201.66 | 0.70/0.00 |
| 162 | 145/2.5/33.33 | 144/2.4/19.42 | -0.69/4.00 | 149 | 142/1.9/18.94 | 143/1.9/22.39 | 0.70/0.00 |
| 1 | 336/0.3/26.83 | 336/0.3/0.63 | 0.00/0.00 | 55 | 140/2.9/8.88 | 141/2.9/22.02 | 0.71/0.00 |
| 2 | 336/0.4/23.27 | 336/0.4/0.64 | 0.00/0.00 | 148 | 140/1.6/20.36 | 141/1.5/11.94 | 0.71/6.25 |
| 4 | 323/1.7/23.27 | 323/1.7/16.08 | 0.00/0.00 | 152 | 135/1.4/8.72 | 136/1.4/10.69 | 0.74/0.00 |
| 24 | 67/1.4/11.54 | 67/1.4/6.72 | 0.00/0.00 | 11 | 265/2.9/28.2 | 267/2.9/56.59 | 0.75/0.00 |
| 27 | 92/2.6/8.81 | 92/2.5/10.97 | 0.00/3.85 | 7 | 263/2.8/23.39 | 265/2.8/59.31 | 0.76/0.00 |
| 30 | 347/1.9/35.91 | 347/1.9/62.39 | 0.00/0.00 | 5 | 255/1.6/18.16 | 257/1.6/23.42 | 0.78/0.00 |
| 34 | 67/1.8/11.89 | 67/1.7/1.72 | 0.00/5.56 | 15 | 254/3.6/26.06 | 256/3.6/77.13 | 0.79/0.00 |
| 38 | 72/2.2/8.77 | 72/2.1/3.22 | 0.00/4.55 | 94 | 126/3/14.83 | 127/2.8/67.3 | 0.79/6.67 |
| 42 | 80/1.7/8.3 | 80/1.6/3.69 | 0.00/5.88 | 8 | 243/2.6/29.36 | 245/2.6/62.44 | 0.82/0.00 |
| 47 | 56/1.9/8.97 | 56/1.8/2.64 | 0.00/5.26 | 171 | 120/3.3/23.28 | 121/3.3/87.58 | 0.83/0.00 |
| 60 | 216/2.5/22.92 | 216/2.5/124.41 | 0.00/0.00 | 169 | 119/3.3/23.64 | 120/3.3/60.06 | 0.84/0.00 |
| 66 | 67/1.9/8.58 | 67/1.8/2.41 | 0.00/5.26 | 53 | 118/2.5/8.97 | 119/2.5/12.23 | 0.85/0.00 |
| 74 | 85/1.9/8.33 | 85/1.9/3.64 | 0.00/0.00 | 41 | 224/2.8/23.22 | 226/2.8/90.05 | 0.89/0.00 |
| 76 | 60/2.6/9.36 | 60/2.6/3.3 | 0.00/0.00 | 23 | 97/1.9/8.73 | 98/1.9/3.72 | 1.03/0.00 |
| 81 | 81/2.3/9.42 | 81/2.1/4.23 | 0.00/8.70 | 32 | 194/2.3/16.45 | 196/2.3/16.03 | 1.03/0.00 |
| 90 | 46/2.4/8.53 | 46/2.4/13.89 | 0.00/0.00 | 29 | 96/1.6/8.47 | 97/1.6/4.52 | 1.04/0.00 |
| 108 | 46/1.7/9.39 | 46/1.7/0.52 | 0.00/0.00 | 209 | 96/2.3/10.17 | 97/2.3/9.86 | 1.04/0.00 |
| 113 | 31/1.1/9.4 | 31/1.1/0.63 | 0.00/0.00 | 210 | 96/2.3/9.41 | 97/2.3/10.48 | 1.04/0.00 |
| 120 | 97/1.9/9.23 | 97/1.9/1.09 | 0.00/0.00 | 213 | 95/2.5/17.77 | 96/2.5/11.97 | 1.05/0.00 |
| 121 | 58/1.8/8.94 | 58/1.8/0.31 | 0.00/0.00 | 214 | 95/2.5/14.69 | 96/2.4/12.69 | 1.05/4.00 |
| 137 | 62/2.7/13.66 | 62/2.7/3.48 | 0.00/0.00 | 212 | 94/2.2/9.86 | 95/2.2/7.8 | 1.06/0.00 |
| 144 | 153/0.5/13.84 | 153/0.5/1.84 | 0.00/0.00 | 215 | 90/2.5/9.95 | 91/2.5/17.08 | 1.11/0.00 |
| 145 | 153/0.6/13.02 | 153/0.6/1.39 | 0.00/0.00 | 13 | 266/3/28.14 | 269/3/58.67 | 1.13/0.00 |
| 146 | 153/0.6/18.63 | 153/0.6/0.45 | 0.00/0.00 | 6 | 261/2.8/32.77 | 264/2.8/58.47 | 1.15/0.00 |
| 147 | 145/1.7/18.86 | 145/1.6/10.52 | 0.00/5.88 | 39 | 174/2.6/13.47 | 176/2.6/31.84 | 1.15/0.00 |
| 150 | 143/2/17.42 | 143/1.9/30.41 | 0.00/5.00 | 85 | 86/1.9/11.66 | 87/1.8/5.25 | 1.16/5.26 |
| 153 | 143/2/8.85 | 143/1.9/24.89 | 0.00/5.00 | 12 | 256/2.4/23.3 | 259/2.4/27.7 | 1.17/0.00 |
| 154 | 140/2.1/13.74 | 140/1.9/22.11 | 0.00/9.52 | 35 | 168/3.6/16.65 | 170/3.6/45.03 | 1.19/0.00 |
| 156 | 137/1.7/8.84 | 137/1.6/22.42 | 0.00/5.88 | 68 | 168/2.6/14.16 | 170/2.6/20.11 | 1.19/0.00 |
| 157 | 136/1.7/20.34 | 136/1.6/17.14 | 0.00/5.88 | 51 | 412/3.6/77.19 | 417/3.6/560.52 | 1.21/0.00 |
| 159 | 139/2/8.88 | 139/2/21.86 | 0.00/0.00 | 206 | 78/3.2/11.33 | 79/3.2/6.34 | 1.28/0.00 |
| 160 | 135/1.9/8.83 | 135/1.7/23.84 | 0.00/10.53 | 33 | 154/3/14.06 | 156/3/54.19 | 1.30/0.00 |
| 161 | 147/2.4/12.13 | 147/2.4/19.5 | 0.00/0.00 | 37 | 374/3.5/48.26 | 379/3.5/682.97 | 1.34/0.00 |
| 163 | 147/2.6/18.78 | 147/2.6/15.33 | 0.00/0.00 | 158 | 138/2/19.23 | 140/1.9/21.92 | 1.45/5.00 |
| 164 | 141/2.2/11.94 | 141/2.2/32.8 | 0.00/0.00 | 31 | 135/2/8.47 | 137/1.8/21.45 | 1.48/10.00 |
| 165 | 111/2.7/13.73 | 111/2.7/36.61 | 0.00/0.00 | 22 | 395/3.5/57.27 | 401/3.5/338.8 | 1.52/0.00 |
| 184 | 105/0.4/14.84 | 105/0.4/0.33 | 0.00/0.00 | 9 | 253/2.5/24.27 | 257/2.5/73.16 | 1.58/0.00 |
| 185 | 105/0.7/9.02 | 105/0.7/0.33 | 0.00/0.00 | 10 | 253/2.5/23.48 | 257/2.5/72.05 | 1.58/0.00 |
| 186 | 105/1.3/8.83 | 105/1.3/0.7 | 0.00/0.00 | 75 | 248/2.6/43.77 | 252/2.6/124.45 | 1.61/0.00 |
| 187 | 105/1.3/8.8 | 105/1.3/0.73 | 0.00/0.00 | 170 | 117/3.2/11.75 | 119/3.2/94.17 | 1.71/0.00 |
| 191 | 105/1.5/8.81 | 105/1.5/2.03 | 0.00/0.00 | 58 | 292/3/38.2 | 297/3/260.61 | 1.71/0.00 |
| 193 | 104/1.6/8.58 | 104/1.6/2.81 | 0.00/0.00 | 54 | 114/2/11.64 | 116/2/7.19 | 1.75/0.00 |

Table 7: Comparing SLIPSA with DaliLite (Continued)

| No. | DaliLite n/r/t | SLIPSA n/r/t | SLIPSA $n^+/r^-$ | No. | DaliLite n/r/t | SLIPSA n/r/t | SLIPSA $n^+/r^-$ |
|---|---|---|---|---|---|---|---|
| 65 | 285/3.4/48.03 | 290/3.4/500.44 | 1.75/0.00 | 67 | 260/6.7/28.1 | 273/6/1084.95 | 5.00/10.45 |
| 123 | 340/2/67.59 | 346/2/192.13 | 1.76/0.00 | 178 | 80/4.1/9.67 | 84/4.1/114.92 | 5.00/0.00 |
| 138 | 55/2.9/8.99 | 56/2.9/2.86 | 1.82/0.00 | 43 | 57/2.6/8.43 | 60/2.6/5.06 | 5.26/0.00 |
| 166 | 106/2.7/13.66 | 108/2.7/36.13 | 1.89/0.00 | 103 | 67/2.8/10.84 | 71/2.8/10.34 | 5.97/0.00 |
| 167 | 106/2.7/8.89 | 108/2.7/33.78 | 1.89/0.00 | 72 | 133/3/13.78 | 141/3/31.47 | 6.02/0.00 |
| 93 | 262/2.6/23.55 | 267/2.6/15.75 | 1.91/0.00 | 199 | 83/3.2/8.85 | 88/3.2/28.22 | 6.02/0.00 |
| 49 | 261/2.7/43.21 | 266/2.7/204.52 | 1.92/0.00 | 129 | 47/2.8/9.86 | 50/2.8/2.98 | 6.38/0.00 |
| 59 | 189/2.9/18.13 | 193/2.9/97.23 | 2.12/0.00 | 101 | 106/4.3/13.58 | 113/4.3/285.97 | 6.60/0.00 |
| 63 | 94/2.6/8.38 | 96/2.3/8.45 | 2.13/11.54 | 78 | 75/3/8.66 | 80/3/15.23 | 6.67/0.00 |
| 70 | 188/2.5/13.92 | 192/2.5/49.75 | 2.13/0.00 | 56 | 114/3.6/14.02 | 122/3.5/117.25 | 7.02/2.78 |
| 48 | 89/2/8.44 | 91/1.9/4.3 | 2.25/5.00 | 89 | 114/3.6/13.63 | 122/3.5/117.34 | 7.02/2.78 |
| 87 | 131/3.1/13.27 | 134/3.1/26.02 | 2.29/0.00 | 62 | 71/3.2/8.77 | 76/3.2/6.34 | 7.04/0.00 |
| 200 | 86/3.4/9.36 | 88/3.4/26.72 | 2.33/0.00 | 105 | 65/3.1/8.83 | 70/3.1/23.09 | 7.69/0.00 |
| 127 | 85/2.9/10.17 | 87/2.9/12.42 | 2.35/0.00 | 135 | 72/3.9/24.28 | 78/3.9/62.7 | 8.33/0.00 |
| 83 | 211/3.5/28.71 | 216/3.5/497.88 | 2.37/0.00 | 182 | 71/3.7/38.27 | 77/3.7/113.52 | 8.45/0.00 |
| 18 | 250/3.4/23.03 | 256/3.4/54.63 | 2.40/0.00 | 224 | 50/3.8/9.7 | 55/3.8/9.66 | 10.00/0.00 |
| 84 | 291/3.3/62.72 | 298/3.3/355.72 | 2.41/0.00 | 77 | 94/3.3/8.52 | 104/3.3/81.64 | 10.64/0.00 |
| 168 | 121/3.5/30.89 | 124/3.5/87.14 | 2.48/0.00 | 132 | 69/2.8/9.05 | 77/2.8/10.5 | 11.59/0.00 |
| 69 | 80/2.1/8.5 | 82/2.1/8.63 | 2.50/0.00 | 96 | 116/5.3/13.34 | 130/5.3/181.38 | 12.07/0.00 |
| 119 | 36/3/10.63 | 37/2.8/0.7 | 2.78/6.67 | 98 | 64/2.2/13.92 | 72/2.2/43.89 | 12.50/0.00 |
| 222 | 71/2.8/9.52 | 73/2.7/23.52 | 2.82/3.57 | 142 | 71/3.2/18.77 | 80/3.2/19.98 | 12.68/0.00 |
| 202 | 69/2.4/8.73 | 71/2.4/6.45 | 2.90/0.00 | 61 | 206/4.1/32.95 | 233/4.1/1182.63 | 13.11/0.00 |
| 106 | 66/3.4/9.08 | 68/3.3/7.59 | 3.03/2.94 | 131 | 67/3.3/22.08 | 76/3.3/8.3 | 13.43/0.00 |
| 107 | 65/3.7/8.59 | 67/3.7/16.09 | 3.08/0.00 | 104 | 81/5.2/14.11 | 93/5.2/108.55 | 14.81/0.00 |
| 141 | 63/3/19.34 | 65/2.8/3.61 | 3.17/6.67 | 183 | 66/6.3/11.77 | 76/6.2/89.92 | 15.15/1.59 |
| 130 | 62/2.9/14.44 | 64/2.8/2.98 | 3.23/3.45 | 109 | 53/3.2/9.66 | 62/3.2/10.36 | 16.98/0.00 |
| 45 | 401/3.1/52.25 | 414/3.1/521.05 | 3.24/0.00 | 177 | 84/7/9.48 | 99/7/700.17 | 17.86/0.00 |
| 174 | 121/3.9/13.66 | 125/3.9/77.64 | 3.31/0.00 | 181 | 83/6.7/13.75 | 98/6.6/649.63 | 18.07/1.49 |
| 172 | 120/3.8/24.03 | 124/3.8/104.23 | 3.33/0.00 | 71 | 82/3.3/8.42 | 98/3.3/38.05 | 19.51/0.00 |
| 57 | 149/3/16.75 | 154/3/95.56 | 3.36/0.00 | 20 | 56/3.4/8.67 | 67/3.4/15.17 | 19.64/0.00 |
| 217 | 89/2.8/14.98 | 92/2.7/19.17 | 3.37/3.57 | 118 | 27/2.5/8.97 | 33/2.4/0.42 | 22.22/4.00 |
| 111 | 59/3.1/9.36 | 61/3.1/7.27 | 3.39/0.00 | 100 | 89/6.6/8.56 | 109/6.5/221.02 | 22.47/1.52 |
| 40 | 147/2.7/13.34 | 152/2.7/21.13 | 3.40/0.00 | 176 | 83/4.4/33.33 | 103/4.4/242.14 | 24.10/0.00 |
| 86 | 114/3.1/8.85 | 118/3.1/29.55 | 3.51/0.00 | 124 | 180/5.2/89.42 | 227/5.2/4821.3 | 26.11/0.00 |
| 175 | 113/3.2/19.06 | 117/3.2/100.83 | 3.54/0.00 | 95 | 101/5.9/23.8 | 131/5.9/659.64 | 29.70/0.00 |
| 73 | 82/2.8/8.83 | 85/2.6/12.73 | 3.66/7.14 | 19 | 99/4.9/13.27 | 129/4.9/314.61 | 30.30/0.00 |
| 112 | 27/2.3/8.67 | 28/2.3/0.88 | 3.70/0.00 | 180 | 71/4.9/17.13 | 93/4.9/171.09 | 30.99/0.00 |
| 125 | 81/2.8/21.94 | 84/2.8/15.56 | 3.70/0.00 | 179 | 79/4.6/14.47 | 108/4.6/312.5 | 36.71/0.00 |
| 143 | 104/3.2/20.03 | 108/3.2/62.34 | 3.85/0.00 | 133 | 47/6.7/9.24 | 67/6.7/19.44 | 42.55/0.00 |
| 79 | 103/3/8.77 | 107/3/77.69 | 3.88/0.00 | 88 | 61/3.8/8.55 | 88/3.8/45.11 | 44.26/0.00 |
| 221 | 77/2.7/24.17 | 80/2.7/14.05 | 3.90/0.00 | 36 | 37/5.3/9.78 | 55/4.6/9.77 | 48.65/13.21 |
| 64 | 74/1.8/8.51 | 77/1.8/18.58 | 4.05/0.00 | 102 | 75/10.3/13.86 | 124/10.3/1903.98 | 65.33/0.00 |
| 97 | 74/1.8/8.39 | 77/1.8/18.5 | 4.05/0.00 | 21 | n/a | / | / |
| 223 | 73/3/9.27 | 76/3/13.47 | 4.11/0.00 | 46 | n/a | / | / |
| 82 | 97/3.2/11.18 | 101/3.2/13.97 | 4.12/0.00 | 80 | n/a | / | / |
| 208 | 97/2.4/13.91 | 101/2.4/13.44 | 4.12/0.00 | 91 | n/a | / | / |
| 134 | 70/3/14.22 | 73/2.8/8.69 | 4.29/6.67 | 99 | n/a | / | / |
| 205 | 70/2.9/14.1 | 73/2.8/10.03 | 4.29/3.45 | 110 | n/a | / | / |
| 204 | 68/2.7/9.54 | 71/2.7/12.2 | 4.41/0.00 | 114 | n/a | / | / |
| 216 | 90/2.8/12.86 | 94/2.7/26.19 | 4.44/3.57 | 115 | n/a | / | / |
| 25 | 88/2.8/8.57 | 92/2.8/10.06 | 4.55/0.00 | 116 | n/a | / | / |
| 220 | 88/2.7/9.56 | 92/2.7/24.88 | 4.55/0.00 | 117 | n/a | / | / |
| 218 | 87/2.5/10.89 | 91/2.5/19.34 | 4.60/0.00 | 122 | n/a | / | / |
| 92 | 105/3.1/11.81 | 110/3.1/82.5 | 4.76/0.00 | 126 | n/a | / | / |
| 139 | 82/3.3/30.33 | 86/3.3/35.14 | 4.88/0.00 | 128 | n/a | / | / |
| 173 | 121/4/13.53 | 127/4/72.64 | 4.96/0.00 | 140 | n/a | / | / |

Table 8: Comparing SLIPSA with SSM

| | SSM | SLIPSA | | | SSM | SLIPSA | |
|---|---|---|---|---|---|---|---|
| No. | n/r/t | n/r/t | $n^+/r^-$ | No. | n/r/t | n/r/t | $n^+/r^-$ |
| 224 | 47/3.16/8.05 | 35/2.97/9.3 | -25.53/6.01 | 185 | 103/0.73/7.16 | 105/0.73/0.42 | 1.94/0.00 |
| 118 | 32/1.49/11.91 | 28/1.44/0.5 | -12.50/3.36 | 52 | 153/1.56/9.27 | 156/1.53/9.86 | 1.96/1.92 |
| 122 | 31/2.85/6.31 | 30/2.73/1.16 | -3.23/4.21 | 191 | 102/1.35/7.6 | 104/1.35/3.92 | 1.96/0.00 |
| 23 | 93/1.31/7.41 | 91/1.25/3.44 | -2.15/4.58 | 193 | 101/1.44/11.73 | 103/1.43/4.28 | 1.98/0.69 |
| 121 | 56/1.5/12.49 | 55/1.45/0.42 | -1.79/3.33 | 144 | 149/0.31/7.39 | 152/0.3/2.64 | 2.01/3.23 |
| 2 | 336/0.36/11.93 | 333/0.36/0.67 | -0.89/0.00 | 13 | 244/2.2/7.55 | 249/2.2/81.25 | 2.05/0.00 |
| 14 | 236/1.94/18.28 | 235/1.93/79.36 | -0.42/0.52 | 29 | 93/1.4/7.19 | 95/1.38/3.08 | 2.15/1.43 |
| 4 | 311/1.38/7.21 | 310/1.38/16.25 | -0.32/0.00 | 148 | 138/1.53/11.69 | 141/1.53/14.95 | 2.17/0.00 |
| 1 | 336/0.33/7.83 | 336/0.33/0.61 | 0.00/0.00 | 108 | 45/1.77/5.69 | 46/1.74/0.64 | 2.22/1.69 |
| 3 | 336/0.46/7.27 | 336/0.46/2.67 | 0.00/0.00 | 26 | 269/2.03/10.49 | 275/2.02/165.38 | 2.23/0.49 |
| 21 | 127/1.83/7.3 | 127/1.8/2.89 | 0.00/1.64 | 55 | 131/2.31/11.52 | 134/2.31/16.77 | 2.29/0.00 |
| 28 | 124/2.04/11.61 | 124/1.88/11.64 | 0.00/7.84 | 100 | 85/3.33/10.17 | 87/3.31/91.92 | 2.35/0.60 |
| 34 | 63/1.38/7.17 | 63/1.32/1.38 | 0.00/4.35 | 78 | 78/3.08/6.34 | 80/2.99/19.84 | 2.56/2.92 |
| 47 | 53/1.39/12.03 | 53/1.26/1.97 | 0.00/9.35 | 175 | 113/3.14/11.77 | 116/3.13/125.08 | 2.65/0.32 |
| 69 | 81/2.08/7.36 | 81/2.04/8.59 | 0.00/1.92 | 32 | 184/1.9/7.91 | 189/1.88/31.75 | 2.72/1.05 |
| 74 | 85/2.14/7.58 | 85/1.9/5.28 | 0.00/11.21 | 201 | 73/3.14/11.11 | 75/2.62/17.3 | 2.74/16.56 |
| 110 | 38/1.27/11.27 | 38/1.25/0.92 | 0.00/1.57 | 70 | 182/2.28/7.66 | 187/2.26/70.36 | 2.75/0.88 |
| 113 | 31/1.11/6.26 | 31/1.11/0.69 | 0.00/0.00 | 54 | 109/1.56/11.59 | 112/1.54/6.86 | 2.75/1.28 |
| 114 | 24/1/14.02 | 24/1/1.27 | 0.00/0.00 | 163 | 138/2.21/8.5 | 142/2.17/24.16 | 2.90/1.81 |
| 115 | 29/1.93/9.65 | 29/1.78/0.95 | 0.00/7.77 | 156 | 134/1.63/7.25 | 138/1.63/32.05 | 2.99/0.00 |
| 119 | 33/0.61/7.54 | 33/0.61/1.03 | 0.00/0.00 | 30 | 333/1.75/7.43 | 343/1.72/65.5 | 3.00/1.71 |
| 129 | 49/2.8/5.75 | 49/2.8/2.64 | 0.00/0.00 | 31 | 132/1.75/7.36 | 136/1.7/20.11 | 3.03/2.86 |
| 145 | 152/0.47/11.47 | 152/0.47/1.78 | 0.00/0.00 | 195 | 98/1.5/10.35 | 101/1.44/5.11 | 3.06/4.00 |
| 146 | 153/0.56/7.25 | 153/0.56/0.63 | 0.00/0.00 | 196 | 98/1.59/7.64 | 101/1.56/6.2 | 3.06/1.89 |
| 153 | 143/1.91/7.55 | 143/1.87/32.06 | 0.00/2.09 | 66 | 65/1.94/7.77 | 67/1.77/2.45 | 3.08/8.76 |
| 157 | 136/1.66/7.14 | 136/1.63/23.78 | 0.00/1.81 | 16 | 225/2.61/7.38 | 232/2.6/89.39 | 3.11/0.38 |
| 192 | 102/1.35/10.33 | 102/1.26/4.73 | 0.00/6.67 | 168 | 120/3.65/7.52 | 124/3.61/102.97 | 3.33/1.10 |
| 194 | 103/1.62/8.8 | 103/1.57/3.95 | 0.00/3.09 | 137 | 57/2.24/7.34 | 59/2.16/4.41 | 3.51/3.57 |
| 219 | 90/2.06/7.94 | 90/2.02/9.48 | 0.00/1.94 | 40 | 141/2.26/7.28 | 146/2.23/20.55 | 3.55/1.33 |
| 161 | 141/2.19/7.7 | 142/2.06/28.34 | 0.71/5.94 | 49 | 246/2.28/7.56 | 255/2.26/103.47 | 3.66/0.88 |
| 154 | 137/1.83/7.59 | 138/1.8/29.59 | 0.73/1.64 | 5 | 241/1.29/11.55 | 250/1.29/19.88 | 3.73/0.00 |
| 155 | 137/1.74/7.48 | 138/1.58/34.03 | 0.73/9.20 | 42 | 76/1.5/5.72 | 79/1.47/3.13 | 3.95/2.00 |
| 152 | 134/1.37/12.2 | 135/1.35/13.67 | 0.75/1.46 | 206 | 76/3.26/13.83 | 79/3.23/9.13 | 3.95/0.92 |
| 53 | 110/1.88/7.17 | 111/1.88/12.06 | 0.91/0.00 | 112 | 25/1.27/9.3 | 26/1.21/0.88 | 4.00/4.72 |
| 184 | 103/0.39/10.02 | 104/0.37/0.48 | 0.97/5.13 | 140 | 98/3.24/8.98 | 102/3.21/22.28 | 4.08/0.93 |
| 186 | 102/1.09/7.22 | 103/1.05/0.89 | 0.98/3.67 | 207 | 98/2.38/10.85 | 102/2.31/11.91 | 4.08/2.94 |
| 187 | 102/1.07/15.32 | 103/1.05/0.95 | 0.98/1.87 | 11 | 240/2.2/10.64 | 250/2.2/86.77 | 4.17/0.00 |
| 188 | 102/1.42/7.49 | 103/1.36/3.16 | 0.98/4.23 | 9 | 238/2.13/7.7 | 248/2.11/41.92 | 4.20/0.94 |
| 189 | 102/1.42/7.55 | 103/1.38/3.17 | 0.98/2.82 | 62 | 70/2.95/5.97 | 73/2.89/7.53 | 4.29/2.03 |
| 190 | 102/1.3/7.54 | 103/1.28/1.09 | 0.98/1.54 | 169 | 115/3.38/14.08 | 120/3.27/94.8 | 4.35/3.25 |
| 197 | 98/1.34/7.55 | 99/1.27/4.92 | 1.02/5.22 | 172 | 115/3.45/9.48 | 120/3.42/96.53 | 4.35/0.87 |
| 198 | 98/1.88/8.38 | 99/1.86/6.59 | 1.02/1.06 | 222 | 69/2.43/11.95 | 72/2.41/16.16 | 4.35/0.82 |
| 212 | 92/1.98/14.97 | 93/1.98/8.28 | 1.09/0.00 | 223 | 69/2.43/7.48 | 72/2.39/22.92 | 4.35/1.65 |
| 27 | 89/2.36/8.19 | 90/2.33/9.47 | 1.12/1.27 | 123 | 311/1.13/9.57 | 325/1.12/225.61 | 4.50/0.88 |
| 39 | 169/2.39/7.3 | 171/2.35/29.41 | 1.18/1.67 | 151 | 133/1.85/8.08 | 139/1.83/24.94 | 4.51/1.08 |
| 125 | 82/2.68/7.03 | 83/2.63/13.41 | 1.22/1.87 | 68 | 155/2.27/11.61 | 162/2.25/23.77 | 4.52/0.88 |
| 93 | 241/1.45/10.39 | 244/1.44/18.23 | 1.24/0.69 | 120 | 88/1.12/7.81 | 92/1.12/1.53 | 4.55/0.00 |
| 81 | 79/2.12/7.14 | 80/2.02/3.95 | 1.27/4.72 | 106 | 65/3.33/6.3 | 68/3.3/10.13 | 4.62/0.90 |
| 158 | 136/1.82/7.18 | 138/1.82/30.92 | 1.47/0.00 | 48 | 85/1.71/11.47 | 89/1.69/4.11 | 4.71/1.17 |
| 159 | 134/1.79/7.23 | 136/1.77/33.52 | 1.49/1.12 | 7 | 231/2/19.33 | 242/1.99/65.95 | 4.76/0.50 |
| 24 | 65/1.35/7.13 | 66/1.32/6.52 | 1.54/2.22 | 79 | 105/3.4/7.44 | 110/3.34/104.19 | 4.76/1.76 |
| 12 | 246/2.04/13.78 | 250/2.04/36.33 | 1.63/0.00 | 75 | 230/2.24/9.74 | 241/2.21/159.78 | 4.78/1.34 |
| 86 | 114/2.85/7.16 | 116/2.84/50.16 | 1.75/0.35 | 25 | 83/2.35/7.23 | 87/2.35/15.66 | 4.82/0.00 |
| 138 | 54/2.75/10.13 | 55/2.68/4.86 | 1.85/2.55 | 76 | 60/2.87/7.56 | 63/2.77/7.59 | 5.00/3.48 |
| 173 | 107/2.91/7.89 | 109/2.87/143.53 | 1.87/1.37 | 60 | 198/2.05/10.56 | 208/2.05/102.94 | 5.05/0.00 |
| 41 | 209/2.36/7.58 | 213/2.34/94.55 | 1.91/0.85 | 80 | 79/2.41/11.66 | 83/2.38/12.05 | 5.06/1.24 |

Table 9: Comparing SLIPSA with SSM (Continued)

| | SSM | SLIPSA | | | SSM | SLIPSA | |
|---|---|---|---|---|---|---|---|
| No. | n/r/t | n/r/t | $n^+/r^-$ | No. | n/r/t | n/r/t | $n^+/r^-$ |
| 150 | 136/1.92/7.44 | 143/1.9/38.11 | 5.15/1.04 | 97 | 70/1.85/11.75 | 77/1.84/19.17 | 10.00/0.54 |
| 58 | 267/2.45/7.58 | 281/2.44/319.89 | 5.24/0.41 | 220 | 80/2.39/7.57 | 88/2.33/27.28 | 10.00/2.51 |
| 6 | 227/1.95/7.56 | 239/1.94/86.83 | 5.29/0.51 | 133 | 49/3.74/5.74 | 54/3.69/10.75 | 10.20/1.34 |
| 164 | 132/2.12/7.39 | 139/2.1/49.83 | 5.30/0.94 | 130 | 58/2.88/7.11 | 64/2.86/6.16 | 10.34/0.69 |
| 174 | 113/3.39/9.53 | 119/3.32/92.55 | 5.31/2.06 | 213 | 84/2.14/10.47 | 93/2.05/19.61 | 10.71/4.21 |
| 142 | 74/3.16/7.43 | 78/3.1/35.72 | 5.41/1.90 | 33 | 137/2.74/7.48 | 152/2.74/47.27 | 10.95/0.00 |
| 208 | 92/2.12/9.05 | 97/2.11/18.27 | 5.43/0.47 | 61 | 202/4.05/10.72 | 225/4.04/813.22 | 11.39/0.25 |
| 132 | 73/2.88/5.69 | 77/2.83/8.8 | 5.48/1.74 | 199 | 79/3.36/7.47 | 88/3.2/27.52 | 11.39/4.76 |
| 10 | 236/2.12/10.67 | 249/2.11/64.05 | 5.51/0.47 | 50 | 227/2.01/7.69 | 253/2.01/87.25 | 11.45/0.00 |
| 84 | 271/2.84/16.17 | 286/2.83/428.7 | 5.54/0.35 | 205 | 67/3.36/7.53 | 75/3.24/15.67 | 11.94/3.57 |
| 38 | 72/3.19/13.58 | 76/2.91/8.22 | 5.56/8.78 | 19 | 108/4.36/11.63 | 121/4.3/330.28 | 12.04/1.38 |
| 43 | 54/2.25/7.16 | 57/2.15/6.17 | 5.56/4.44 | 22 | 329/2.47/13.32 | 370/2.47/523.75 | 12.46/0.00 |
| 209 | 90/2.11/9.83 | 95/2.06/10.86 | 5.56/2.37 | 202 | 64/2.51/11.82 | 72/2.48/10.19 | 12.50/1.20 |
| 82 | 89/2.33/7.33 | 94/2.27/10.19 | 5.62/2.58 | 218 | 80/2.39/17.89 | 90/2.39/27.78 | 12.50/0.00 |
| 214 | 88/2.17/7.64 | 93/2.17/12.88 | 5.68/0.00 | 217 | 77/2.43/7.56 | 87/2.37/29.69 | 12.99/2.47 |
| 117 | 35/3.57/7.77 | 37/3.13/12.08 | 5.71/12.32 | 37 | 323/2.99/7.67 | 365/2.98/712.13 | 13.00/0.33 |
| 211 | 87/1.88/18.94 | 92/1.85/12.31 | 5.75/1.60 | 124 | 146/3.28/11 | 166/3.21/2676.58 | 13.70/2.13 |
| 136 | 52/2.39/13.16 | 55/2.28/14.63 | 5.77/4.60 | 139 | 71/2.74/7.32 | 81/2.67/32.8 | 14.08/2.55 |
| 147 | 137/1.64/7.58 | 145/1.62/13.66 | 5.84/1.22 | 95 | 89/3.13/12.67 | 102/3.06/258.66 | 14.61/2.24 |
| 35 | 153/3.15/7.29 | 162/3.13/41 | 5.88/0.63 | 94 | 109/2.67/18 | 125/2.61/84.16 | 14.68/2.25 |
| 105 | 66/3.12/7.19 | 70/3.11/36.42 | 6.06/0.32 | 20 | 61/4.14/7.27 | 70/3.91/18.38 | 14.75/5.56 |
| 8 | 214/1.98/9 | 227/1.96/71.78 | 6.07/1.01 | 71 | 70/1.98/7.38 | 81/1.95/15.67 | 15.71/1.52 |
| 170 | 115/3.45/9.31 | 122/3.45/117.59 | 6.09/0.00 | 109 | 57/4.29/10.73 | 66/4.08/18.52 | 15.79/4.90 |
| 127 | 82/2.97/7.22 | 87/2.88/14.48 | 6.10/3.03 | 57 | 131/2.99/7.39 | 152/2.95/69.23 | 16.03/1.34 |
| 166 | 97/2.46/7.33 | 103/2.43/38.45 | 6.19/1.22 | 107 | 56/3.67/7.27 | 65/3.54/20.75 | 16.07/3.54 |
| 160 | 126/1.75/7.23 | 134/1.69/35.91 | 6.35/3.43 | 92 | 93/2.97/7.34 | 108/2.96/80.75 | 16.13/0.34 |
| 17 | 219/2.29/11.67 | 233/2.27/91.05 | 6.39/0.87 | 36 | 43/4/8.13 | 50/3.94/11.34 | 16.28/1.50 |
| 141 | 61/2.94/7.08 | 65/2.82/4.47 | 6.56/4.08 | 176 | 83/3.98/9.03 | 97/3.93/224.13 | 16.87/1.26 |
| 87 | 121/2.69/7.48 | 129/2.67/56.39 | 6.61/0.74 | 83 | 188/3.81/7.58 | 221/3.78/595.67 | 17.55/0.79 |
| 90 | 45/2.6/10.41 | 48/2.55/20.91 | 6.67/1.92 | 203 | 62/2.86/8.19 | 73/2.86/9.8 | 17.74/0.00 |
| 210 | 90/2.11/15.58 | 96/2.11/11.59 | 6.67/0.00 | 101 | 101/4.75/7.33 | 119/4.73/331.2 | 17.82/0.42 |
| 149 | 134/1.91/10.19 | 143/1.87/28.72 | 6.72/2.09 | 73 | 69/2.28/13.66 | 82/2.22/9.97 | 18.84/2.63 |
| 45 | 371/2.69/7.63 | 396/2.68/542.58 | 6.74/0.37 | 85 | 73/2.1/7.41 | 87/1.82/7.97 | 19.18/13.33 |
| 98 | 73/2.93/7.44 | 78/2.93/70.36 | 6.85/0.00 | 182 | 67/3.88/7.33 | 80/3.88/129.41 | 19.40/0.00 |
| 111 | 58/3.25/9.35 | 62/3.23/10.09 | 6.90/0.62 | 135 | 60/3.27/7.35 | 72/3.24/62.58 | 20.00/0.92 |
| 72 | 130/2.94/7.57 | 139/2.94/36.45 | 6.92/0.00 | 177 | 65/4.41/9.55 | 78/4.37/169.52 | 20.00/0.91 |
| 64 | 69/1.69/7.19 | 74/1.65/16.47 | 7.25/2.37 | 167 | 90/2.81/7.23 | 109/2.79/64.45 | 21.11/0.71 |
| 143 | 109/3.93/7.19 | 117/3.88/80.41 | 7.34/1.27 | 88 | 65/3.26/7.41 | 79/3.25/60.22 | 21.54/0.31 |
| 51 | 375/3.07/11.72 | 403/3.04/549.48 | 7.47/0.98 | 181 | 55/3.2/12.02 | 67/3.11/100.33 | 21.82/2.81 |
| 162 | 132/2.27/11.63 | 142/2.22/29.97 | 7.58/2.20 | 179 | 87/4.6/11.95 | 106/4.53/377.38 | 21.84/1.52 |
| 204 | 66/2.73/8.05 | 71/2.71/17.03 | 7.58/0.73 | 103 | 58/2.85/9.13 | 72/2.78/17.91 | 24.14/2.46 |
| 171 | 113/3.39/9.58 | 122/3.39/191.53 | 7.96/0.00 | 134 | 59/3.23/7.28 | 74/3.08/17.8 | 25.42/4.64 |
| 65 | 251/2.85/8.91 | 271/2.84/312.78 | 7.97/0.35 | 67 | 185/4.02/13.11 | 236/4.02/1101.73 | 27.57/0.00 |
| 165 | 99/2.43/7.28 | 107/2.42/52.7 | 8.08/0.41 | 183 | 33/1.66/7.44 | 43/1.58/15.91 | 30.30/4.82 |
| 59 | 170/2.36/7.45 | 184/2.33/273.2 | 8.24/1.27 | 96 | 75/2.92/10.13 | 103/2.89/119.3 | 37.33/1.03 |
| 18 | 204/2.19/7.3 | 221/2.19/128.86 | 8.33/0.00 | 180 | 56/3.82/7.66 | 77/3.8/159.19 | 37.50/0.52 |
| 56 | 108/3.11/11.92 | 117/3.06/88.72 | 8.33/1.61 | 178 | 50/3.03/8.88 | 72/3.03/89.19 | 44.00/0.00 |
| 89 | 108/3.11/7.55 | 117/3.06/112.03 | 8.33/1.61 | 102 | 45/3.08/7.55 | 68/3.03/206.2 | 51.11/1.62 |
| 216 | 84/2.52/7.69 | 91/2.48/19.88 | 8.33/1.59 | 116 | 20/2.15/7.86 | 31/2.04/3.7 | 55.00/5.12 |
| 215 | 83/2.39/7.72 | 90/2.39/36.94 | 8.43/0.00 | 77 | 44/2.49/10.66 | 92/2.46/63.05 | 109.09/1.20 |
| 104 | 70/2.97/11.98 | 76/2.96/87.03 | 8.57/0.34 | 44 | n/a | / | / |
| 200 | 81/3.71/14.19 | 88/3.39/30.55 | 8.64/8.63 | 46 | n/a | / | / |
| 15 | 212/2.7/12.91 | 231/2.68/101.19 | 8.96/0.74 | 91 | n/a | / | / |
| 131 | 66/2.94/7.57 | 72/2.87/8.28 | 9.09/2.38 | 99 | n/a | / | / |
| 63 | 87/2.4/5.72 | 95/2.01/8.17 | 9.20/16.25 | 126 | n/a | / | / |
| 221 | 72/2.59/11.95 | 79/2.54/17.33 | 9.72/1.93 | 128 | n/a | / | / |